

**(2,2-Dimethylcyclopropyl)carbonyl Grignard Reagents
and the Reactivity of Osmium Tetraoxide and
Peroxy-carboxylic Acids with Low Valent Iridium Compounds**

Thesis by
Jay Douglas Audett

In Partial Fulfillment of the Requirements
for the Degree of
Doctor of Philosophy

California Institute of Technology
Pasadena, California
1984

(Submitted August 17, 1983)

ACKNOWLEDGMENTS

There are several people that I would like to acknowledge for their contributions to my stay at Caltech. Special thanks go to my advisors, J. D. Roberts and Terry Collins, for their patient guidance, and to the departmental policies which accommodated my changing pursuits. The assistance of Bernard Santarsiero and his instruction on the power of X-ray crystallography was appreciated. Mega-thanks are extended to George Harvey Spies who solved the iridium-osmium structure despite the tert-butyl and phenyl decorations.

It is impossible to thank all of the people that helped make my sojourn at Caltech more enjoyable. The members of the Kiwi group (especially Sam Hill) were a congenial crew. The realization of the American dream -- the road trip phenomenon -- was aided by the founding of the A.A.S.S. Special tribute is given to those pioneering founding fathers: Dr. Duck Hillhouse, Babs Thompson, and Leon Spinks Gelles. Many backpacking trips were enjoyed with Terry Smith, Pete Wolczanski, Mark Hiawatha Paffett, Tommy Zeitlow, Steve Hentges, and Jeff Gelles. Fortification for these trips provided by Jimmy Narducci will always be appreciated.

I would like to thank Dot Lloyd for the patient preparation of this manuscript, and finally my parents for their support and encouragement.

ABSTRACT

The formation and rearrangement of Grignard reagents from (2,2-dimethylcyclopropyl)carbinyl halide have been studied. The Grignard reagent from the chloride, 2,2-dimethyl-3-butenyl-1-magnesium chloride, demonstrates the carbanionic influence on the Grignard rearrangement. The bromide yielded no Grignard reagents, only the disproportionated hydrocarbons 4-methyl-1-pentene and 2-methyl-1,4-pentadiene. The dominating radical side reactions for the bromide may be attributed to the weaker carbon-bromine bond which gives rise to complete bond rupture accompanying single-electron transfer from magnesium.

The reactions of several oxidizing agents with Vaska's complex and its derivatives have been investigated. Interesting results with osmium tetroxide and peroxycarboxylic acids are described. Osmium tetroxide reacts with Vaska's complex in the presence of pyridine to form a dinuclear, bridging carbon dioxide complex. Characterization is accomplished with ^{13}C , ^{31}P , and ^1H NMR, in addition to infrared labeling studies. Derivatization of this complex with methyl trifluoromethanesulfonate resulted in O-methylation of the carbon dioxide moiety giving the structurally characterized dinuclear carbene complex. The reaction of peroxycarboxylic acids with Vaska's complex under a variety of conditions has yielded a series of compounds. When Vaska's complex is exposed to at least two equivalents of peroxycarboxylic acid, carbon monoxide is oxidized to carbon dioxide and the iridium product is chlorobis(m-chlorobenzoato)bis(triphenylphosphine)-

iridium(III). When the reaction is performed in the presence of excess tetrafluoroboric acid, carbon monoxide oxidation is prevented and the observed product is chloro(m-chlorobenzoato)carbonylbis(triphenylphosphine)iridium(III) tetrafluoroborate. The p-methylbenzoato analogue of this compound has been structurally characterized, and the reactions of nucleophiles with these iridium cations are described. The series of reactions performed with peroxy-carboxylic acid suggest a previously unconsidered mechanism for the formation of chlorobis(m-chlorobenzoato)bis(triphenylphosphine)iridium(III) from Vaska's complex and the peroxy-carboxylic acid.

TABLE OF CONTENTS

	<u>Page</u>
SECTION 1: Grignard Reactions	1
CHAPTER I. (2,2-Dimethylcyclopropyl)carbinyl Grignard Reagents	3
SECTION 2: The Reactivity of Oxidizing Agents with Organometallic Compounds	32
CHAPTER II: Osmium Tetraoxide	37
CHAPTER III: Peroxycarboxylic Acid	72

SECTION 1: Grignard Reactions

An understanding of the formation and rearrangements of Grignard reagents has been achieved by studying the reaction of (2,2-dimethylcyclopropyl)carbinyl halide with magnesium. The chloride yielded 2,2-dimethyl-3-butenyl-1-magnesium chloride which demonstrated the carbanionic influence on the Grignard rearrangement. The bromide did not give any Grignard products. It instead did radical side reactions such as disproportionation as demonstrated by the identification of 4-methyl-1-pentene and 2-methyl-1,4-pentadiene. This reactivity indicates radical intermediacy in Grignard reagent formation. The dominating radical side reactions for the bromide may be attributed to the weaker carbon-bromine bond which gives rise to complete bond rupture accompanying single-electron transfer from magnesium.

CHAPTER I

(2,2-Dimethylcyclopropyl)carbonyl Grignard Reagents

Introduction

Grignard reagents have been used in chemical syntheses for almost a century. The discovery and development of this useful and versatile reagent earned Victor Grignard the Nobel prize in 1912. It is surprising that, despite its years of widespread use, an adequate understanding of the mechanism of its formation has only recently been achieved. The reason for the delay is the difficulty in acquiring reliable data for the heterogeneous reaction of an alkyl halide with a magnesium surface.

During the past decade, evidence has accumulated supporting an electron-transfer mechanism. Such a process can give rise to intermediate radicals that can ultimately yield Grignard compounds or radical side products. The ease and cleanliness of Grignard reagent preparation will depend primarily upon the alkyl halide and its degree of adsorption on the magnesium surface. If the alkyl halide is strongly adsorbed, any radical intermediacy will probably give Grignard products as opposed to radical side-reaction pathways such as disproportionation or coupling.

Recent workers have managed to overcome problems relevant to acquiring kinetic data for Grignard formation.¹ By using magnesium rods attached to a high torque, adjustable speed stirrer, they were able to obtain reproducible kinetics for a variety of alkyl chlorides, bromides, and iodides. They concluded that the rate of reaction is proportional to organic halide concentration and magnesium surface area. This implies that the reaction occurs at the solution-magnesium interface. Most organic bromides and iodides react with magnesium at either mass-transport and/or diffusion-limited rates. Alkyl chlorides react at least a hundred times slower than

expected for a transport-limited process, and their structure-reactivity profiles are qualitatively similar to the profiles of alkyl bromides which do not react at transport-limited rates. This suggests a similar mechanism for these two classes of halides. The rate-structure profiles rule out mechanisms involving carbonium ions, carbanions, or S_N2 processes. From this accumulated data, Whitesides concludes that it is difficult to choose between halogen abstraction or generation of an alkyl halide radical anion by single-electron transfer as the initial step of carbon-halogen bond cleavage. In fact, electron transfer would promote bond cleavage. Formation of an alkyl radical as the key intermediate of the reaction has been suggested by others, based on the observation of CIDNP in the NMR spectra of Grignard reactions.² Formation of intermediate radicals would be expected to be feasible following electron-transfer from magnesium to the alkyl halide.

Another study consistent with the electron-transfer mode of reactivity involved comparison of Hammett ρ -values for the reactions of aryl halides with magnesium versus with tri-*n*-butyltin hydride.³ This work leaves three possibilities open. These include the already mentioned electron-transfer mechanism generating a radical anion, bromine abstraction by magnesium forming an aryl radical, or direct insertion of magnesium into the carbon-bromine bond of the aryl bromide. These three possibilities are not mutually exclusive. Electron-transfer may precede or occur coincidentally with bromine abstraction or magnesium insertion.

The observation of CIDNP signals in the 1H NMR during the formation of Grignard reagents implies that some of the Grignard product derives from radical precursors. Because the extent of nuclear polarization is unknown, it

is not clear whether these CIDNP studies reflect the major pathway for formation of Grignard reagent or a minor side reaction. By using cleverly designed radical traps, Whitesides has shown that at least 80% of cyclopentylmagnesium bromide is formed via radical intermediates.⁴ The difficulty in using a radical trap such as 2,2,6,6-tetramethylpiperidine nitroxyl (TMPO) is its reactivity with Grignard reagents. However, tert-butyl alcohol was employed to scavenge any Grignard formed, so that the TMPO present can only react with intermediate radicals. By optimizing the concentrations of tert-butyl alcohol and TMPO, it was shown that more than 80% of the Grignard reagent arose from radical intermediates. Walborsky conjectures an electron-transfer process from the metal surface precedes radical formation.⁵ He concludes that electron transfer occurs from magnesium to make Grignard reagents and from lithium in synthesizing alkyllithiums.

In preparing Grignard reagents, common side reactions include Wurtz coupling and radical pathways. The Grignard reagent from 1-adamantyl (1-Ad) bromide is difficult to synthesize as radical side reactions dominate. The three suggested pathways diverging from the common transient intermediate are illustrated below (Figure 1).⁶

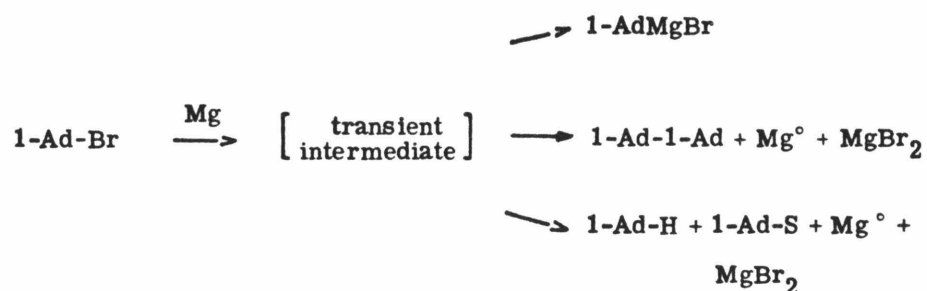


Figure 1

The workers conclude that the formation of Grignard reagents depends upon the degree of adsorption of the alkyl halide to the magnesium surface. Good yields of Grignard reagents are obtained for systems in which the alkyl halide has a high adsorption and for which an outer-sphere process is operative. For alkyl halides which are poorly adsorbed, yields can be improved by using less polar solvents with no stirring. Otherwise, the radical side reactions such as reaction with solvent, disproportionation, or coupling dominate.

The ease of electrochemical reduction of alkyl halides parallels their reactivities with magnesium metal.⁷ It is probable that Grignard reagent formation proceeds via electron transfer into the σ^* carbon-halogen antibonding orbital of the alkyl halide. Depending upon the halide, the carbon-halogen bond lengthening accompanying this electron transfer may vary from slight to complete rupture. In the case of complete rupture, the alkyl radicals generated can yield Grignard reagent or undergo the radical side reactions previously indicated.

An interesting approach to studying Grignard reagents is to use the cyclopropylcarbinyl rearrangement system (Figure 2). Radical or carbonium ion character would favor the tertiary component (C), and carbanionic character is expected to yield the primary components (A and B). The extent that B is observed depends upon the degree to which the Thorpe-Ingold effect will stabilize B relative to the open-chain component A. The extent of radical intermediacy in Grignard reagent formation should be determinable by product analysis. Radical intermediacy would favor initial formation of the Grignard reagent C or products derivable from the corresponding radical.

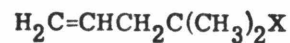
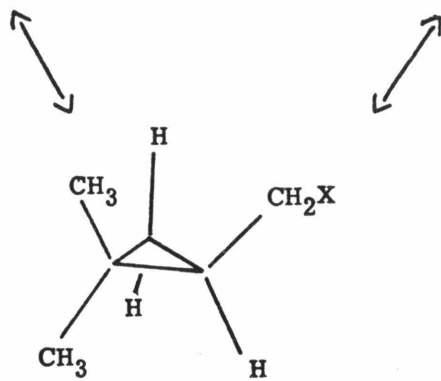
ACB

Figure 2

An additional interesting feature of this system is the rearrangements which occur for the corresponding Grignard reagents. The interconversion of cyclopropylcarbinyl and allylcarbinyl Grignard reagents has been established over past years.⁸ For rearrangement of the parent system, shown below, the half-life of cyclopropylcarbinylmagnesium bromide is 121 minutes at -24°C and is a first-order reaction (Figure 3).⁸

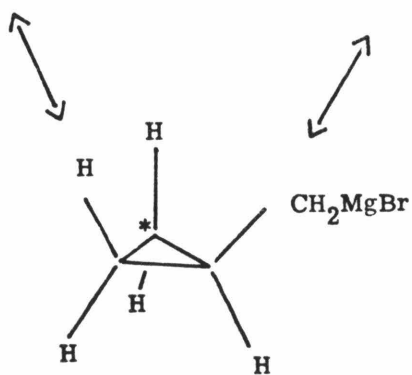
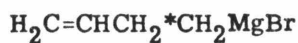


Figure 3

In the formation of Grignard reagents of this system, the initial product from the cyclopropylcarbinyl halide or from the allylcarbinyl halide appears to contain both cyclic and open-chain compounds.⁸ This is consistent with rearrangement during formation of the Grignard reagent, probably via radical intermediates. The energy difference between the cyclopropylcarbinyl Grignard reagent and the open-chain reagent is approximately 7 kcal/mol⁸ and can be reduced by stabilizing the cyclopropyl ring with the introduction of geminal alkyl groups.⁹ If four methyl groups are placed on the cyclopropyl ring, the Grignard reagent exists 99.9% in the cyclic form because of stabilization of the cyclopropane structure and destabilization of the open-chain reagent.¹⁰ In this system, the open-chain Grignard reagent is tertiary and destabilized relative to the primary Grignard cyclopropyl structure (Figure 4).

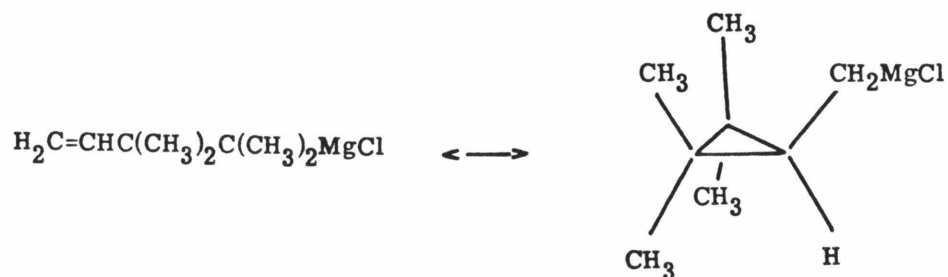


Figure 4

The rearrangement to the primary Grignard reagent argues strongly for the carbanionic nature of the carbon-magnesium bond in Grignard reagents.

The system investigated in the current studies has two methyl groups on the cyclopropane ring (Figure 5).

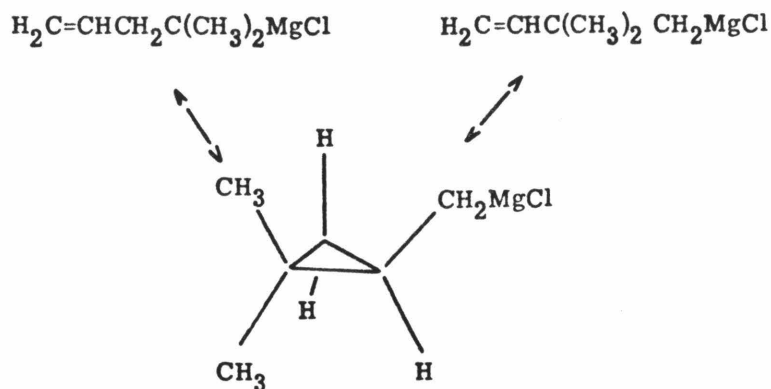


Figure 5

When the tertiary Grignard reagent is prepared from the chloride in tetrahydrofuran, it rearranges with a half-life of 30 hours at 70°C.¹⁰ At equilibrium, 99.9% of the primary 3-butenyl Grignard reagent is obtained compared to 0.07% of the cyclopropylcarbinyl Grignard compound.¹⁰ The further investigation of this rearrangement has been undertaken by attempting the direct synthesis of the intermediate (2,2-dimethylcyclopropyl)carbinyl Grignard compound and studying its properties.

Results

The synthesis and rearrangement of (2,2-dimethylcyclopropyl)carbinylmagnesium halide was studied to determine the extent to which radicals or carbanions are involved. (2,2-Dimethylcyclopropyl)carbinyl chloride was prepared and proven a successful precursor to the Grignard reagent only at room temperature. Rearrangement to the open-chain, primary Grignard reagent occurred quickly at this temperature, and this negated the possibility

No Grignard reagent could be obtained from (2,2-dimethylcyclopropyl)carbinyl bromide as judged by the absence of acidic components after quenching the reaction mixture with dry ice. The volatile alkenes obtained from this reaction indicated intermediacy of radicals which disproportionate rather than yield Grignard products. The two products consistently obtained from this reaction were 4-methyl-1-pentene and 2-methyl-1,4-pentadiene, in addition to higher molecular weight polymers. Evidence was obtained for the presence of 4,4,5,5-tetramethyl-1,7-octadiene and 3,3-dimethyl-1-butene in one trial. The nearly one-to-one ratio of 4-methyl-1-pentene and 2-methyl-1,4-pentadiene indicates the following mechanistic scheme (Figure 7). The 3,3-dimethyl-1-butene may have arisen from cyclopropyl ring opening to yield the primary radical, or from hydrolysis of trace amounts of 2,2-dimethyl-3-butenyl-1-magnesium bromide.

The proposed radical scheme is in agreement with recent work on the mechanism of Grignard reagent formation involving single-electron transfer to the halide to give a radical anion which subsequently reacts with magnesium to yield the Grignard reagent (Figure 8).¹⁻⁷ In the case of the chloride, the Grignard reagent is obtained and none of the disproportionation alkenes are observed; while, for bromide, the carbon-halogen bond lengthening process accompanying single-electron transfer is increased by the bromide. The bond lengthening is increased to the point of bond rupture before the magnesium insertion step can occur (Figure 9).

The cyclopropylcarbinyl radical opens entirely to yield the tertiary radical rather than the primary radical. The tertiary radical subsequently undergoes disproportionation and other radical side reactions. The direction

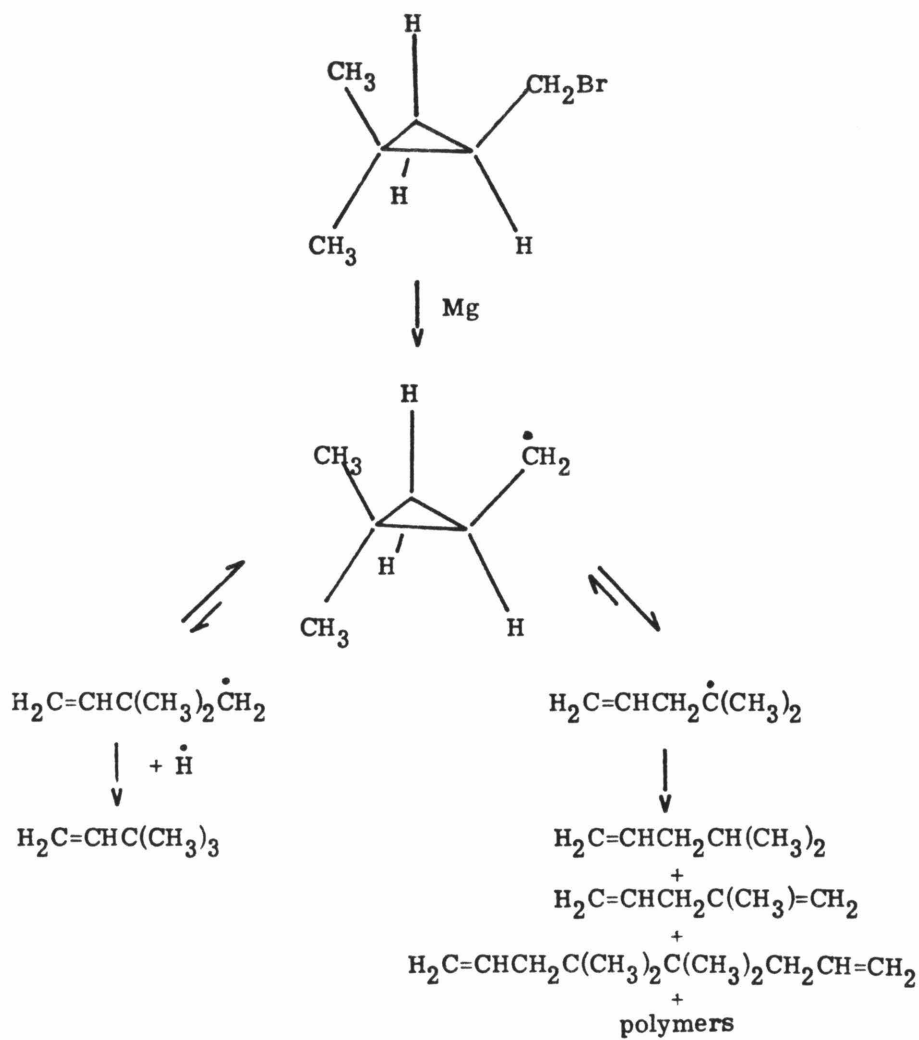


Figure 7

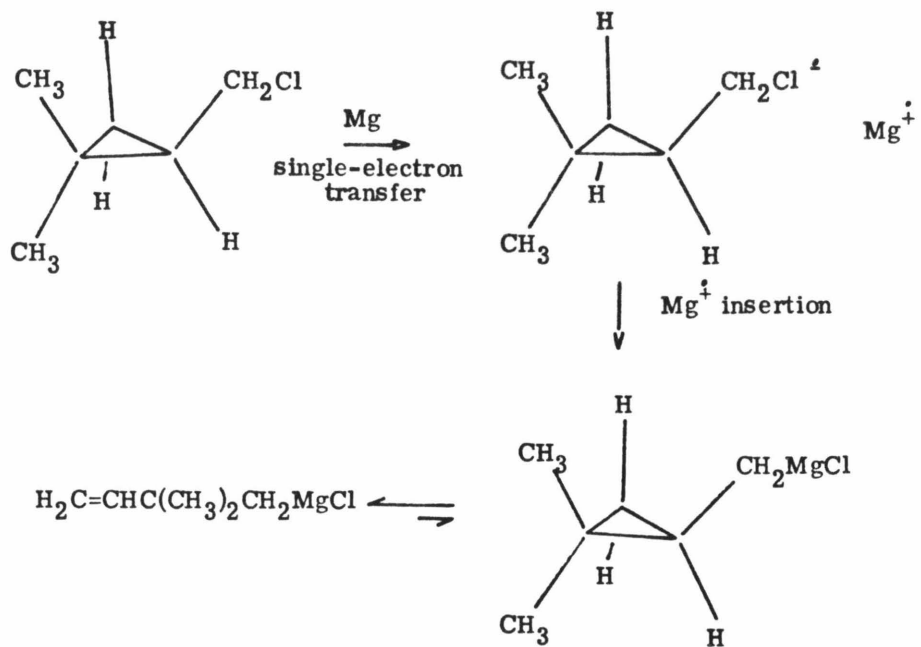


Figure 8

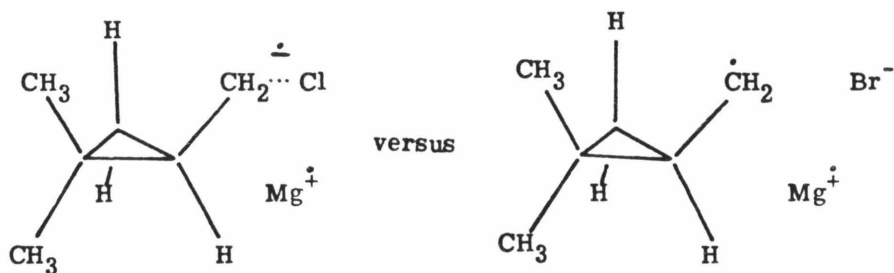


Figure 9

of the cyclopropylcarbinyl radical ring opening is in accord with electronic and steric factors.¹¹ Conclusive proof for this radical scheme is provided by generation of the radicals from the bromide with tri-*n*-butyltin hydride. In this experiment, the same alkene, 4-methyl-1-pentene, is obtained. This alkene arises from generation of the cyclopropylcarbinyl radical with subsequent ring opening to yield the stabilized tertiary radical. The opened radical then abstracts hydrogen from the tin hydride to continue the chain reaction (Figure 10).

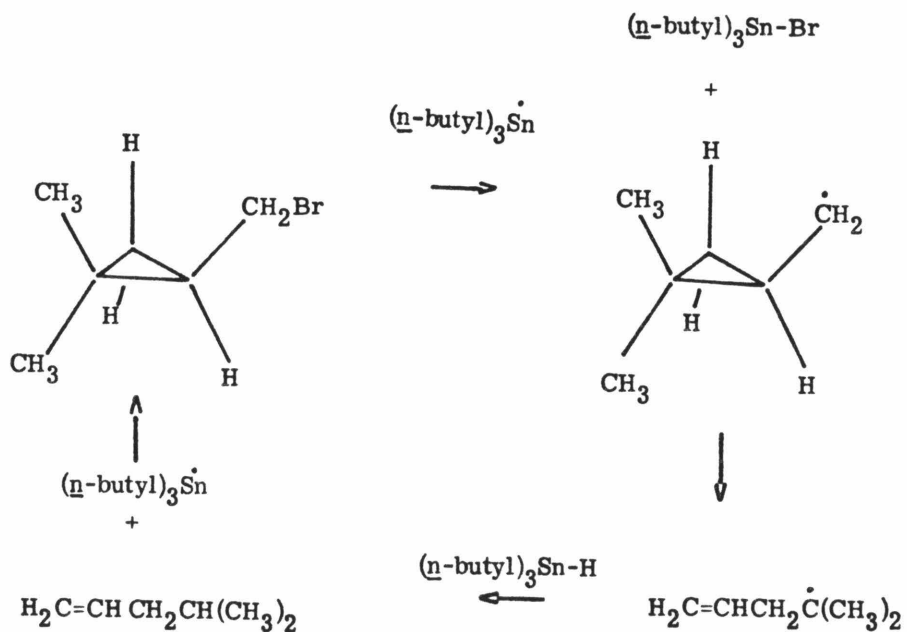


Figure 10

Rearrangement of the bromide catalyzed by magnesium bromide which evolves under Grignard formation conditions is a minor pathway (Pathway I, Figure 11). At 0°C in the presence of magnesium bromide, the cyclopropylcarbinyl bromide rearranges much slower than the rate of reaction of the bromide with magnesium to generate the cyclopropylcarbinyl radical (Pathway II, Figure 11).

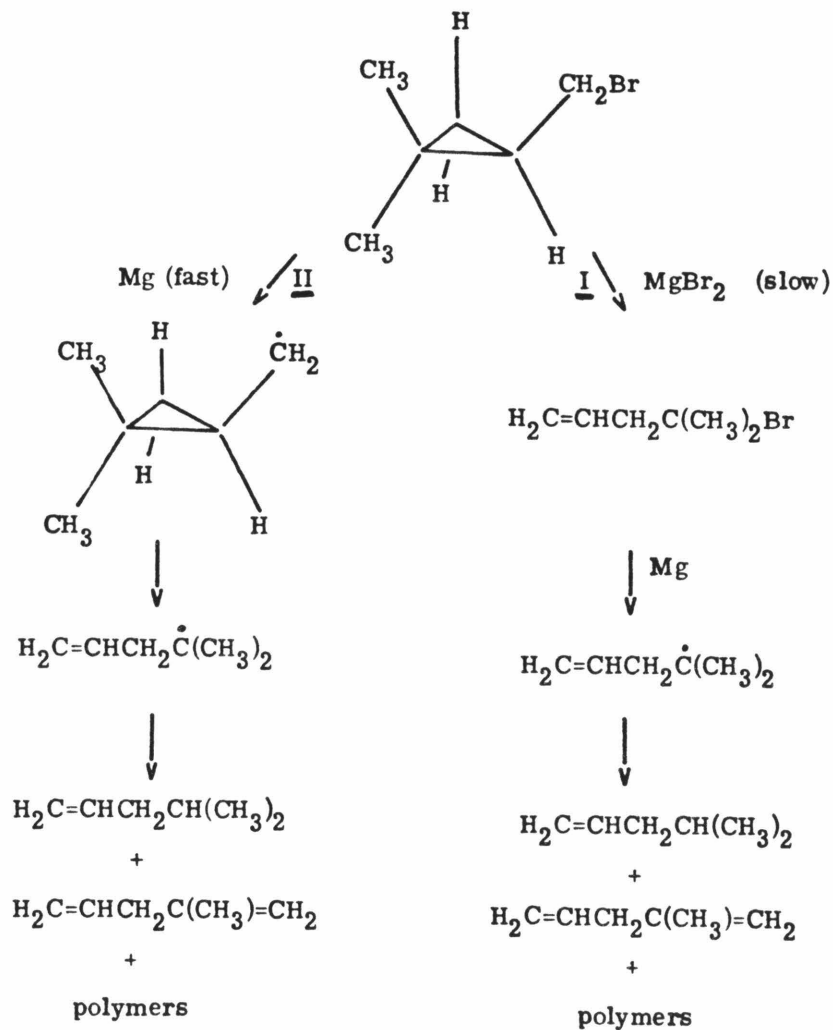


Figure 11

If some of the starting bromide does rearrange to 2-bromo-2-methyl-4-pentene, preparation of the Grignard reagent from 2-bromo-2-methyl-4-pentene will yield the same alkenes as pathway II so that the two pathways are indistinguishable using product analysis.

The behavior of the radical with regard to cyclopropyl ring opening is opposite the direction of ring opening observed for the chloride Grignard reagent. This is conclusive proof for the carbanionic nature of the Grignard reagent rearrangement (Figure 12). Path II for ring opening is observed with the radical prepared with tri-*n*-butyltin hydride. This is expected since it yields the energetically favored tertiary radical. The Grignard reagent prepared from (2,2-dimethylcyclopropyl)carbinyl chloride ring opened via path III. The opposite direction of ring opening observed here via the energetically favored primary carbanion is strong evidence for the carbanionic nature of the Grignard rearrangement.

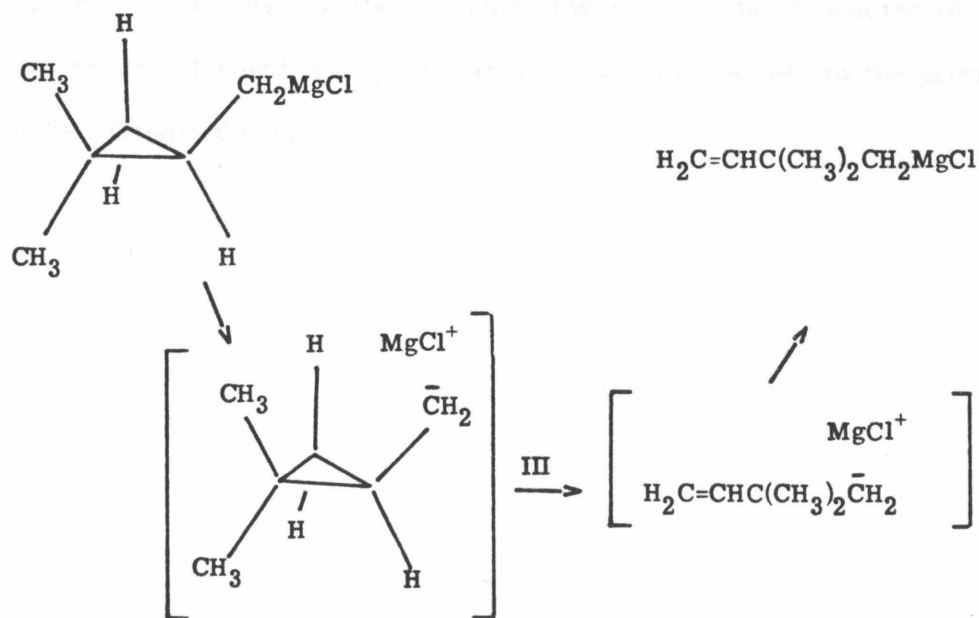


Figure 12

This argument assumes that the cyclopropyl Grignard reagent is initially generated followed by rapid conversion to the primary open-chain reagent. If the rearrangement occurred during Grignard reagent formation, this would be expected to occur via a radical pathway. Radical rearrangement prior to Grignard formation would yield some of the tertiary Grignard reagent. This species is sufficiently long-lived to yield some 2,2-dimethyl-4-pentenoic acid upon carbonation.¹⁰ Because this acid is not observed, the cyclopropyl Grignard must be generated initially (Figure 13).

By studying both the chloride and bromide of this cyclopropylcarbonyl system, evidence supporting radical intermediacy in Grignard reagent formation has been obtained. In the case of the bromide, radical side reactions supersede Grignard reagent formation. The dominating radical side reactions may be attributed to the weaker carbon-bromine bond which gives rise to complete bond breaking accompanying single-electron transfer from magnesium. In the case of the chloride, the carbanionic character of the Grignard reagent formed results in rearrangement exclusively to the primary ring-opened Grignard reagent.

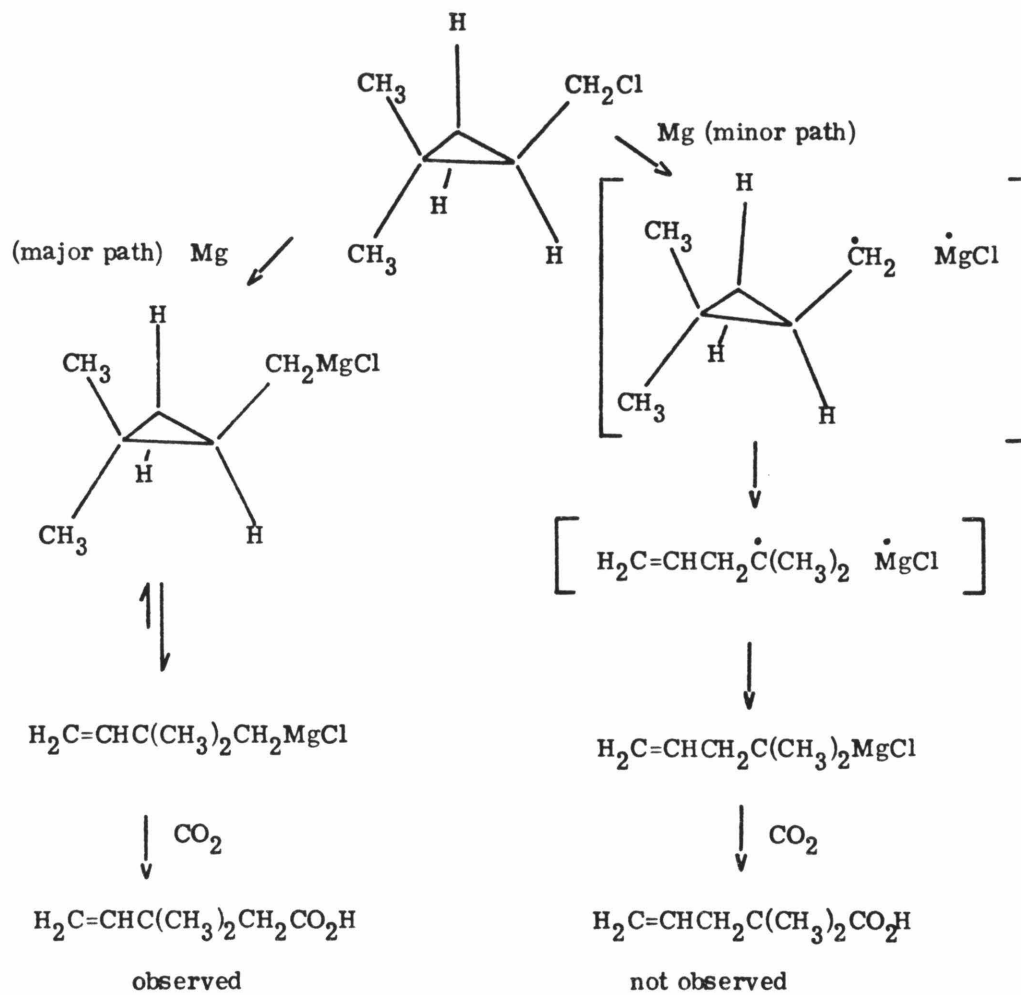


Figure 13

Experimental Section

Preparation of the Ditosylate of 2,2-Dimethyl-1,3-propanediol. The ditosylate was prepared according to Nelson.¹² A solution of 2,2-dimethyl-1,3-propanediol (20.0 g) in 38.5 mL of pyridine was added dropwise to *p*-toluenesulfonyl chloride (110 g) dissolved in 192 mL of pyridine. The addition was conducted at 0°C with stirring. After the mixture was allowed to stand at room temperature overnight, it was poured into ice and water. The white solid was suction filtered and washed with distilled water, dilute sulfuric acid, dilute sodium carbonate, and again with water. Recrystallization from acetone-water gave 65 g of the ditosylate (82%): mp 121°C.

Preparation of 2,2-Dimethylcyclopropane Nitrile. The nitrile was prepared in accord with Nelson.¹² The ditosylate of 2,2-dimethyl-1,3-propanediol (61.8 g) and potassium cyanide (29.34 g) were stirred at 100°C in 300 mL ethylene glycol for 1 h. The reaction temperature was then increased to 200°C. The distillate was collected over a boiling range of 150°C to 198°C. The nitrile phase of the distillate was separated from the ethylene glycol phase. The ethylene glycol was extracted with *n*-pentane. The *n*-pentane extracts and nitrile phase were combined, and the *n*-pentane distilled under reduced pressure. The residual nitrile (8.6 g, 60%) was judged pure by gas chromatography, and the ¹H NMR spectrum was in agreement with the assigned structure (Table 1, Entry 1).

Preparation of 2,2-Dimethylcyclopropanecarboxylic Acid. This acid was synthesized in accord with Nelson¹² except that the optimum base concentration for the nitrile hydrolysis and the workup conditions had to be determined. In the hydrolysis, 2,2-dimethylcyclopropane nitrile (12.8 g) was

heated to reflux in 100 mL of 10 M potassium hydroxide for 60 h. The reaction mixture was poured slowly into an ice and sulfuric acid mixture. The upper organic layer was separated and the aqueous phase was extracted with diethyl ether. The extracts and organic layer were combined and dried with magnesium sulfate. The ether was evaporated and the acid distilled under reduced pressure at 100°C (25 mm Hg). The yield was 13 g (85%). A ¹H NMR spectrum consistent with the structure was obtained (Table 1, Entry 2).

Preparation of (2,2-Dimethylcyclopropyl)carbinol. In a 500-mL flask was placed 250 mL of anhydrous ether and 7.6 g of lithium aluminum hydride. 2,2-Dimethylcyclopropanecarboxylic acid (13 g) dissolved in 20 mL of anhydrous ether was added slowly to maintain gentle reflux. The mixture was stirred an additional hour, the flask then cooled in ice, and water slowly added until heat was no longer evolved. Some additional ether was required during the hydrolysis to allow stirring to be maintained. Then, 180 mL of 10% dilute sulfuric acid was added, and the ether layer was separated and dried with magnesium sulfate. Extraction of the aqueous layer with ether yielded no further product. The ether was removed and the crude alcohol was distilled (9.4 g, 82%) under reduced pressure at 60-70°C (25 mm Hg). The ¹H NMR spectrum was consistent with the structure of (2,2-dimethylcyclopropyl)carbinol (Table 1, Entry 3).

Preparation of (2,2-Dimethylcyclopropyl)carbonyl Chloride. The reaction was run in accord with Magid.¹³ Triphenylphosphine (1.4 g) and 10 mL of anhydrous ether were added to a flame-dried 50-mL round-bottomed flask. The flask and contents were cooled to -78°C, and 2 mL of hexachloroacetone was added. The mixture was stirred for 5 min and

0.5 g of (2,2-dimethylcyclopropyl)carbinol was injected. The whole stirred at -78°C for 1 h. The ether was removed on the rotary evaporator, and the remaining volatile chlorides were flash distilled under reduced pressure from the solid residue. The ^1H NMR spectrum of the chlorides showed 70% (2,2-dimethylcyclopropyl)carbiny chloride and 20% 2-chloro-2-methyl-4-pentene (Table 1, Entry 4).

When the reaction was carried out at higher temperatures, poorer yields of the desired (2,2-dimethylcyclopropyl)carbiny chloride were obtained. The chloride mixture isomerized to 2-chloro-2-methyl-4-pentene over zinc chloride.

Separation of the chloride mixtures was achieved with a 20' 30% SE-30 on Chromosorb P column. Injections of 0.5 mL were made with a 1.5 mL/sec flow rate, an injection temperature of 130°C , a column temperature of 110°C , and a detector temperature of 80°C . (2,2-Dimethylcyclopropyl)carbiny chloride was collected with 3% contamination by 2-chloro-2-methyl-4-pentene. The chloride was stored at -78°C to prevent isomerization.

Preparation of Tribromoacetophenone. Tribromoacetophenone was prepared in three steps without purification of the intermediate bromides.

The monobromide was prepared in accord with Organic Syntheses.¹⁴ To a flame-dried flask was added acetophenone (50 g) in 50 mL of anhydrous ether. The solution was cooled to 0°C and aluminum trichloride (0.5 g) was added, followed by the slow addition of 67 g of bromine. Upon completion of the addition, the ether and hydrogen bromide were removed. The residue was dissolved in ether and washed with water. The ether was dried with magnesium sulfate and removed on the rotary evaporator. The residue was

used for the next step.

The dibromide was synthesized in accord with Evans and Brooks.¹⁵ The monobromide residue (20 g) was dissolved in 100 mL of boiling chloroform, and 10 g of bromine dissolved in 30 mL of chloroform was added slowly. The chloroform was removed upon completion of bromine addition. The residue was dissolved in ether, washed with dilute sodium carbonate, and dried with magnesium sulfate. After removal of the ether, the residue is used for the final bromination.

Tribromoacetophenone was prepared in accord with Krohnke.¹⁶ The dibromide residue (175 g) was dissolved in 700 mL of glacial acetic acid and sodium acetate (105 g) was added. The mixture was heated and 100 g of bromine was added slowly. Upon consumption of all bromine, the solution was diluted with water and extracted with ether. The ether extracts were combined, washed with water, and dried with magnesium sulfate. The ether was removed, and the residue recrystallized twice from methanol. The yield was 140 g (95%): mp 65°C.

Preparation of (2,2-Dimethylcyclopropyl)carbinyl Bromide. (2,2-Dimethylcyclopropyl)carbinol (2 g) was added to 25 mL of anhydrous ether. Triphenylphosphine (5.84 g) was dissolved in the solution, followed by the addition of tribromoacetophenone (8 g). Formation of an orange mass accompanied the exothermic reaction. The mixture was stirred for 6 h at room temperature. The solid residue was filtered and washed with ether. The resulting ether solution of the bromide was vacuum-transferred with gentle heating. Following evaporation of the ether, a ¹H NMR spectrum showed 95% of the desired bromide. The major impurity was 2-bromo-2-methyl-4-pentene

(Table 1, Entry 5). To avoid isomerization of the bromide, it was freshly prepared prior to each Grignard attempt and stored at -78°C .

Reaction of (2,2-Dimethylcyclopropyl)carbinyl Chloride with Magnesium. Magnesium (0.5 g) and a magnetic stir bar were added to a three-neck flask equipped with condenser, addition funnel, nitrogen inlet, and drying tube. The entire apparatus was flame-dried under nitrogen flow. The apparatus was cooled to room temperature and 10 mL of anhydrous ether was added to the flask. An ice bath was placed around the flask, and 97% (2,2-dimethylcyclopropyl)carbinyl chloride (1.4 g) dissolved in 3 mL of anhydrous ether was added. A small crystal of iodine was added, and the mixture stirred at 0°C for 2 h. With no sign of Grignard formation, the reaction was brought to room temperature. After 30 min, the solution appeared cloudy, and stirring was continued for another 45 min. The reaction mixture was poured over dry ice, and dilute sulfuric acid added. The mixture was extracted with ether. The ether was extracted with 10% potassium hydroxide. The potassium hydroxide fractions were combined and acidified with dilute sulfuric acid. The resulting carboxylic acid was extracted with ether. The ether was dried with magnesium sulfate and evaporated. The residue was dissolved in carbon tetrachloride, and the ^1H NMR spectrum was consistent with the structure 3,3-dimethyl-4-pentenoic acid (Table 1, Entry 6).

Gas chromatographic analysis of the reaction solution using an SE-30 column at 60°C showed that the alkenes, 4-methyl-1-pentene and 2-methyl-1,4-pentadiene were not present.

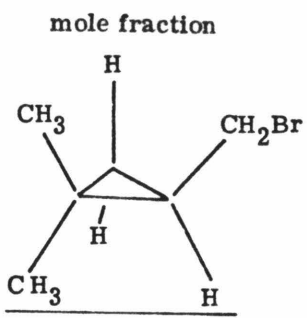
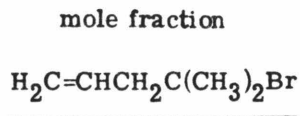
Reaction of (2,2-Dimethylcyclopropyl)carbinyl Bromide with

Magnesium. Magnesium (0.5 g) and a magnetic stir bar were added to a flask equipped with an argon gas inlet. The apparatus was flame-dried under argon flow. The flask was cooled to 0°C, and 15 mL of anhydrous ether was added. (2,2-Dimethylcyclopropyl)carbiny bromide (0.8 g) was injected. The mixture turned cloudy, then green. Thirty min after the addition, quenching the reaction with carbon dioxide failed to produce any acidic components. Gas chromatographic analysis using a 20' SE-30 on Chromosorb P column at 60°C showed four components: 1.00 part 4-methyl-1-pentene, 0.95 parts 2-methyl-1,4-pentadiene, and traces of 3,3-dimethyl-1-butene and 4,4,5,5-tetramethyl-1,7-octadiene. These compounds were collected and identified by their ¹H NMR spectra (Table 1, Entries 7-10). Polymeric material was also obtained from the reaction.

Three repetitions of the above procedure yielded 2-methyl-1,4-pentadiene and 4-methyl-1-pentene in approximately a one-to-one ratio, free of 3,3-dimethyl-1-butene and 4,4,5,5-tetramethyl-1,7-octadiene.

Rearrangement of (2,2-Dimethylcyclopropyl)carbiny Bromide over Magnesium Bromide. A magnesium bromide solution was prepared by the reaction of 1,2-dibromoethane with magnesium in anhydrous ether under an argon atmosphere. Approximately 1.3 M magnesium bromide was prepared and cooled to 0°C. (2,2-Dimethylcyclopropyl)carbiny bromide (0.5 g) was added to 15 mL of the magnesium bromide solution, and the isomerization followed by periodically adding aliquots to excess pentane to precipitate the magnesium bromide. The magnesium bromide was removed by filtration, and the solvents evaporated. ¹H NMR spectra were obtained of the bromide mixtures. The ratio of bromides was determined by integration of the

methyl signals of the two predominant components, (2,2-dimethylcyclopropyl)carbinyl bromide and 2-bromo-2-methyl-4-pentene (Table 1, Entries 5 and 11).

time (minutes)		
0	0.90	0.10
10	0.82	0.18
180	0.00	1.00

Reaction of 2-Bromo-2-methyl-4-pentene with Magnesium. The Grignard procedure for (2,2-dimethylcyclopropyl)carbinyl bromide was repeated, except 2-bromo-2-methyl-4-pentene was used instead of the cyclopropyl bromide. No acidic products were obtained upon carbonation of the mixture. Gas chromatographic analysis demonstrated the presence of one part 4-methyl-1-pentene and 0.76 parts 2-methyl-1,4-pentadiene. Polymeric materials were also present. A 20' SE-30 on Chromosorb P column at 60°C was used.

Preparation of the 2,2-Dimethylcyclopropylcarbinyl Radical. A drop of benzene, 0.5 g tri-n-butyltin hydride, and 0.28 g (2,2-dimethylcyclopropyl)carbinyl bromide were added to an NMR tube. Bubbles

appeared as the sample was irradiated 20 min with a 200-watt mercury-xenon lamp. Gas chromatographic analysis of the solution showed 4-methyl-1-pentene (99%) and 2-methyl-1,4-pentadiene (1%). A 20' SE-30 on Chromosorb P column at 60°C was used. This result demonstrated rapid cyclopropylcarbinyl radical ring opening to yield the tertiary radical.

Photolysis of (2,2-dimethylcyclopropyl)carbinyl bromide dissolved in benzene did not result in rearrangement of the bromide, insuring that the product of the tri-n-butyltin hydride photolysis was the result of the usual radical pathway and not a photoreaction of the bromide.

Table 1. ^1H NMR Data

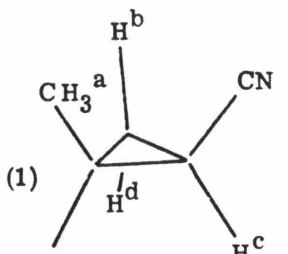
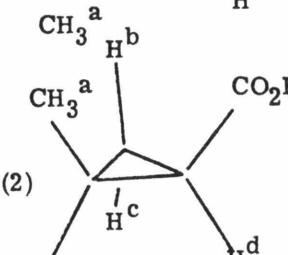
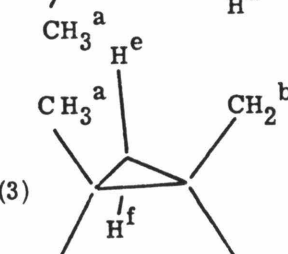
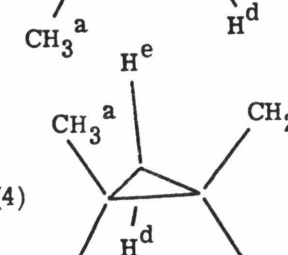
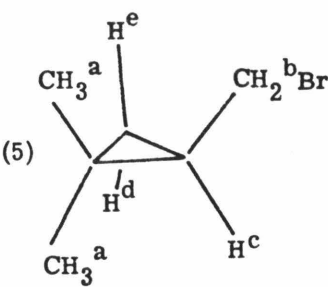
Compound	Solvent	H^x	δ	Intensity	$^3J_{\text{H}-\text{H}}$
 <p>(1)</p>	CCl_4	a b, c, d	1.4, 1.45 1.2-1.5	6 3	two singlets complex multiplet
 <p>(2)</p>	neat	a b, c, d e	1.5, 1.6 1.1-1.9 not observed	6 3	two singlets complex multiplet
 <p>(3)</p>	CCl_4	a b c d e f	1.0, 1.1 3.50 3.8 0.8 0.4 0.05	6 2 1 1 1 1	two singlets eight lines singlet multiplet four lines three lines
 <p>(4)</p>	CCl_4	a b c d e	1.1, 1.15 3.5 1.0 0.25 0.60	6 2 1 1 1	two singlets eight lines multiplet three lines four lines
$\text{H}_2\text{C}=\text{CH}^d\text{CH}_2^b\text{C}(\text{CH}_3^a)_2\text{Cl}$	CCl_4	a b c d	1.55 2.4 5.0 5.9	6 2 2 1	singlet doublet (7Hz) multiplet multiplet

Table 1. Continued

<u>Compound</u>	<u>Solvent</u>	<u>H^x</u>	<u>δ</u>	<u>Intensity</u>	<u>³J_{H-¹H}</u>
(5) 	CCl ₄	a	1.15, 1.2	6	two singlets
		b	3.4	2	eight lines
		c	1.1	1	multiplet
		d	0.3	1	three lines
		e	0.75	1	four lines
(6) H ₂ ^e C=CH ^d C(CH ₃ ^a) ₂ CH ₂ ^b CO ₂ H ^c	CCl ₄	a	1.25	6	singlet
		b	2.4	2	singlet
		c	10	1	broad
		d	5.9	1	four lines
		e	5.0	2	three lines
(7) H ₂ ^c C=CH ^b C(CH ₃ ^a) ₃	CCl ₄	a	0.95	9	singlet
		b	5.5-5.9	1	four lines
		c	4.7-4.9	2	multiplet
(8) H ₂ ^e C=CH ^d CH ₂ ^c CH ^b (CH ₃ ^a) ₂	CCl ₄	a	0.95	6	doublet (7Hz)
		b	1.7	1	multiplet
		c	1.9	2	multiplet
		d	5.7	1	multiplet
		e	4.95	2	two broad lines
(9) H ₂ ^d C=CH ^c CH ₂ ^b C(CH ₃ ^a)=CH ₂ ^d	CCl ₄	a	1.7	3	singlet
		b	2.75	2	doublet (6Hz)
		c	5.6	1	multiplet
		d	4.6-5.0	4	three broad lines
(10) $\left[\text{H}_2^{\text{d}}\text{C}=\text{CH}^{\text{c}}\text{CH}_2^{\text{b}}\text{C}(\text{CH}_3^{\text{a}})- \right]_2$	CCl ₄	a	0.85	6	singlet
		b	1.95	2	doublet (6Hz)
		c	5.7	1	multiplet
		d	4.7-5.0	2	three broad lines
(11) H ₂ ^d C=CH ^c CH ₂ ^b C(CH ₃ ^a) ₂ Br	CCl ₄	a	1.75	6	singlet
		b	2.65	2	doublet (6Hz)
		c	6.0	1	multiplet
		d	5.2	2	multiplet

References and Notes

- (1) (a) Rogers, H. R.; Hill, C. L.; Fujiwara, Y.; Rogers, R. J.; Mitchell, H. L.; Whitesides, G. M. J. Am. Chem. Soc. **1980**, 102, 217. (b) Rogers, H. R.; Deutch, J.; Whitesides, G. M. Ibid. **1980**, 102, 226.
- (2) (a) Walborsky, H. M.; Aronoff, M. S. J. Organomet. Chem. **1973**, 51, 31. (b) Walborsky, H. M.; Young, A. E. J. Am. Chem. Soc. **1964**, 86, 3288.
- (3) Rogers, H. R.; Rogers, R. J.; Mitchell, H. L.; Whitesides, G. M. J. Am. Chem. Soc. **1980**, 102, 231.
- (4) Lawrence, L. M.; Whitesides, G. M. J. Am. Chem. Soc. **1980**, 102, 2493.
- (5) Walborsky, H. M.; Banks, R. B. Bull. Soc. Chim. Belg. **1980**, 89, 849.
- (6) Molle, G.; Bauer, P.; Dubois, J. E. J. Org. Chem. **1982**, 47, 4120.
- (7) (a) Fleischmann, M.; Pletcher, D.; Vance, C. S. J. Electroanal. Chem. **1971**, 29, 325. (b) Bays, J. P.; Blumer, S. T.; Baral-Tosh, S.; Benar, D.; Neta, P. J. Am. Chem. Soc. **1983**, 105, 320.
- (8) (a) Patel, D.; Hamilton, C.; Roberts, J. D. J. Am. Chem. Soc. **1965**, 87, 5144. (b) Mazur, R.; Roberts, J. D. Ibid. **1951**, 73, 2509. (c) Silver, M.; Shafer, P.; Nordlander, J.; Ruchardt, C.; Roberts, J. D. Ibid. **1960**, 82, 2646
- (9) (a) Ingold, C.; Thorpe, J. J. Chem. Soc. **1915**, 107, 1080. (b) Ingold, C. Ibid. **1921**, 119, 305. (c) Stevenson, A.; Thorpe, J. Ibid. **1922**, 121, 650. (d) Allinger, N.; Zalkow, V. J. Org. Chem. **1960**, 25, 701. (e) Good, W.; Hill, E. A.; Link, D. C.; Donn-delinger, P. Ibid. **1981**, 46, 1177.

- (10) Maercker, A. Angew. Chem. Int. Ed., Engl. **1973**, 12, 774.
- (11) Mariano, P.; Bay, E. J. Org. Chem. **1980**, 45, 1763.
- (12) Nelson, E. R.; Maienthal, M.; Lane, L. A.; Benderly, A. A. J. Am. Chem. Soc. **1957**, 79, 3467.
- (13) Magid, R. M.; Fruchey, O. S.; Johnson, W. L.; Allen, T. G. J. Org. Chem. **1979**, 44, 359.
- (14) Blatt, A. H. "Organic Syntheses, Collective Volume II"; John Wiley and Sons: New York, 1944; p. 480.
- (15) Evans, W. L.; Brooks, B. T. J. Am. Chem. Soc. **1908**, 30, 404.
- (16) Krohnke, F. Ber. **1936**, 69, 921.

**SECTION 2: The Reactivity of Oxidizing Agents
With Organometallic Compounds**

A number of oxidants have been investigated in this work to determine reactivities with organometallic compounds. A goal of this work is the development of selective oxidation chemistry for organometallic compounds. Possible modes of oxidation in these systems include (1) electron-transfer pathways, (2) metal oxidation resulting from oxidative addition reactions, and (3) ligand oxidation.

Our interest in the oxidation chemistry available to organometallic compounds involves ligation changes in the organometallic substrate which result from ligand oxidation or an oxidative addition reaction of the oxidant. The study of electron-transfer pathways which do not result in substantial coordinative changes is not desired. An example is the outer-sphere process below (Figure 1).¹



Figure 1

There are several examples of selective ligand oxidation in the literature. Iodosobenzene can be used to oxidize carbon monoxide to carbon dioxide. It has also been used to generate a formaldehyde complex via nucleophilic attack on a cationic methyldene complex (Figure 2).²

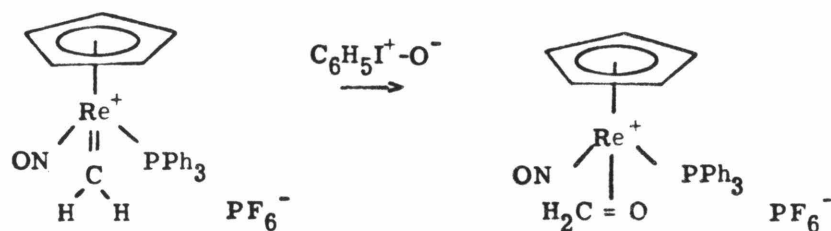


Figure 2

An example of an oxidative addition reaction is the reaction of iodine with Vaska's complex (Figure 3).

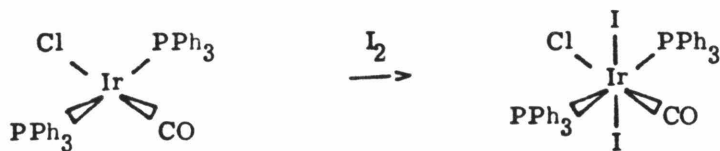


Figure 3

Oxygen similarly oxidizes Vaska's complex (Figure 4).

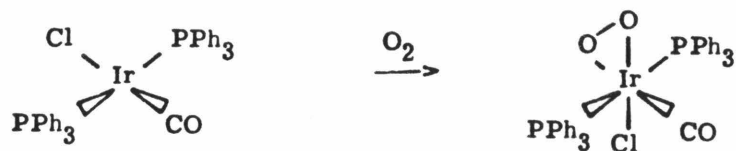


Figure 4

Two of the oxidizing agents that have been examined in this work are peroxycarboxylic acids and osmium tetroxide. Because the organic chemistry of both reagents is selective, their application as organometallic oxidants seems promising. Peroxycarboxylic acids have long been used for the conversion of alkenes into epoxides. Osmium tetroxide is used for the catalytic conversion of alkenes into cis-diols.

An example of a non-selective oxidant is ozone which oxidizes not only the metal center, but also oxidizable ligands on organometallic compounds. For example, introduction of ozone to Vaska's complex results in oxidation of carbon monoxide and triphenylphosphine to give an uncharacterizable mixture.

The organometallic compounds used in these studies are Vaska's complex and its derivatives. This square-planar d^8 compound is ideal for reactions with oxidizing agents because it can undergo oxidative addition reactions, and it contains the oxidizable ligands carbon monoxide and triphenylphosphine.

Additional oxidants that have been investigated include aryl nitrile N-oxides, o-iodosobenzoic acid, other iodine(III) reagents, and ozone. Benzonitrile N-oxides displayed reactivity with Vaska's complex similar to literature accounts.³ The reaction of o-iodosobenzoic acid with trans-acetone nitrile carbonyl bis(triphenylphosphine)iridium(I) perchlorate resulted in oxidation of carbon monoxide and coordination of two carboxylato ligands. A formulation for this compound consistent with infrared and analytical data is shown below (Figure 5).⁴

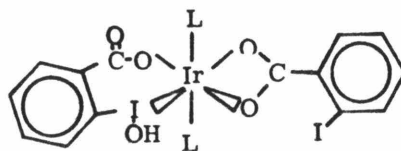


Figure 5

References and Notes

- (1) Cotton, F. A.; Wilkinson, G. "Advanced Inorganic Chemistry"; Interscience Publishers: New York, 1972; p. 673.
- (2) Buhro, W. E.; Patton, A. T.; Strouse, C. E.; Gladysz, J. A. J. Am. Chem. Soc. **1983**, 105, 1056.
- (3) Beck, W.; Keubler, M.; Leidl, E.; Nagel, U.; Schaal, M.; Cenini, S.; Buttero, P.; Licandro, E.; Maiorana, S.; Villa, A. J. Chem. Soc., Chem. Commun. **1981**, 446.
- (4) The infrared spectrum demonstrated the presence of a bidentate carboxylato ligand (ν_a at 1490 cm^{-1} and ν_s at 1420 cm^{-1}) and a monodentate carboxylato ligand (ν_a at 1650 cm^{-1} and ν_s at 1310 cm^{-1}). The elemental analysis was consistent with the proposed formulation. Calculated: C, 48.91; H, 3.20. Found: C, 48.69; H, 3.44.

CHAPTER II

Osmium Tetraoxide

Introduction

The organic oxidation chemistry of osmium tetroxide has been well established over the years.¹ It is the most effective reagent for the cis-hydroxylation of alkenes, and is also commonly used for staining biological tissues. Both uses involve attack of osmium tetroxide at unsaturated functionalities.

In its reactions with alkenes, it has been proposed that osmium tetroxide initially attacks the olefin via direct oxygen attack illustrated in the cyclic transition state below (Figure 1).²⁻⁴

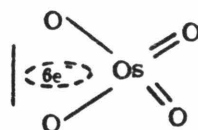


Figure 1

More recently, Sharpless and coworkers expect that the weakly nucleophilic olefin would attack at the electropositive osmium center, forming an initial organometallic intermediate (Figure 2).⁵

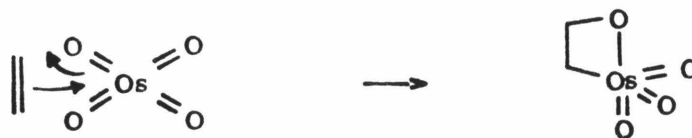


Figure 2

In the presence of tertiary amines, (L), the reaction proceeds to give the well-characterized diolatodioxobis(amine)osmium(VI) ester complexes (Figure 3).⁶

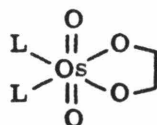


Figure 3

These complexes readily undergo oxidative hydrolysis to yield cis-diols and regenerate osmium tetraoxide.

An ideal organometallic substrate for osmium tetraoxide is Vaska's complex. Square planar iridium(I) compounds readily undergo oxidative addition reactions to give octahedral iridium(III) compounds. In alkene oxidations, the osmium(VIII) tetraoxide undergoes a net two-electron reduction to give the isolable diolatodioxobis(amine)osmium(VI) esters. This two-electron redox compatibility is expected to give clean reactivity.

Results

The reaction of Vaska's complex with osmium tetraoxide in the presence of 4-tert-butylpyridine affords the orange-brown, bridging carbon dioxide adduct I (Figure 4). Other pyridine derivatives may be used, but 4-tert-butylpyridine leads to the most tractable product. The reaction of osmium tetraoxide with Vaska's complex is analogous to alkene-osmium

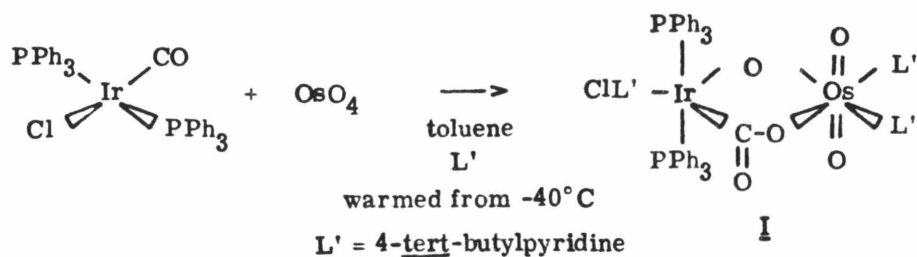


Figure 4

tetraoxide reactivity if the alkene carbon-carbon bond in the diolato-dioxobis(amine)osmium(VI) esters is replaced by the iridium-carbon bond in compound **I**. Because double oxo-bridged species are well established structural entities, it is noteworthy that attack on the carbon monoxide ligand occurred rather than formation of the double oxo-bridged species below (Figure 5).⁷

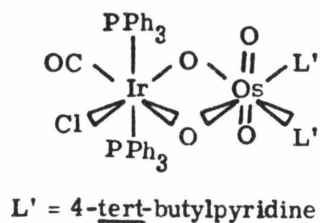


Figure 5

The characterization of compound **I** is best accomplished using NMR and infrared analysis. The osmium(VI) fragment is comparable in its infrared

properties to the diolatodioxobis(amine)osmium(VI) ester complexes. The asymmetric stretch of the trans-dioxo moiety has been positively identified in the infrared spectrum with oxygen-18 labeling. The fate of the carbon monoxide ligand has been established by the infrared spectrum. Conversion to the bridging carbon dioxide ligand follows from a strong carbonyl stretch, $\nu(\text{C}=\text{O})$, at 1593 cm^{-1} which shifts to 1560 cm^{-1} with carbon-13 carbon monoxide. The C-O stretch, $\nu(\text{C}-\text{O})$, is observed to shift from 1022 cm^{-1} to 1010 cm^{-1} with either oxygen-18 or carbon-13 substitution. The ^{13}C NMR signal for the bridging carbon dioxide appears as a triplet with 7 Hz coupling to the phosphorous nuclei which suggests that the triphenylphosphine ligands on iridium are equivalent. The ^1H NMR spectrum shows that the product has three 4-tert-butylpyridines because the tert-butyl protons appear between 1 and 2 δ . It is uncertain with these data whether chloride or 4-tert-butylpyridine is trans to the bridging carbon dioxide ligand.

The dinuclear, bridging carbon dioxide complex is the best characterized example of this bonding mode of carbon dioxide in the literature.⁸ A variety of carbon dioxide adducts have been structurally characterized in the past ten years. Several structures have demonstrated η_2 -carbon dioxide bonding (Figure 6).^{9,10}



Figure 6

Carbon dioxide also gives a head-to-tail coupling product with the iridium compound pictured below (Figure 7).¹¹

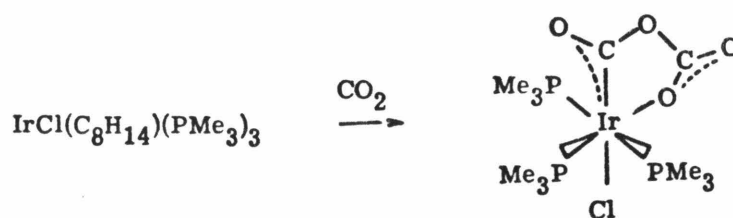


Figure 7

An osmium carbon dioxide cluster complex and a polymeric cobalt carbon dioxide complex have also been structurally characterized.^{12,13} These complexes are similar to the dinuclear carbon dioxide complex reported here except the carbon dioxide in these has a metal associated with each atom. In the polymeric cobalt complex, potassium ions are associated with the oxygens, and, in the osmium complex, an osmium is associated with each atom (Figure 8).

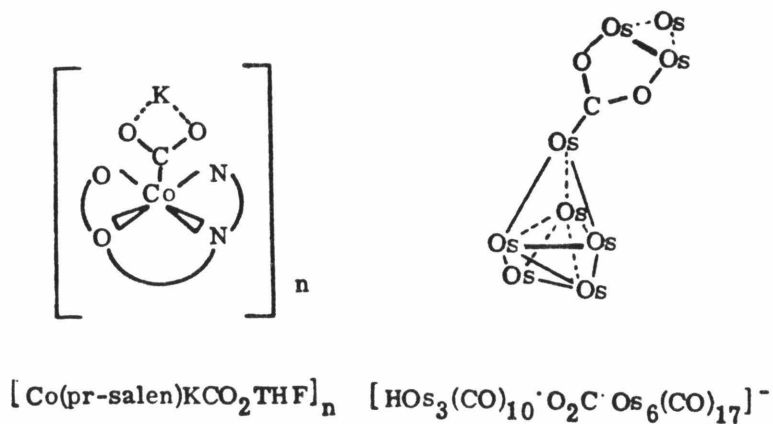


Figure 8

The structure of our dinuclear complex lends support to recent work by Floriani in which a similar structure is proposed as an intermediate for the conversion of carbon dioxide to carbon monoxide and a bridging oxo ligand (Figure 9).¹⁴

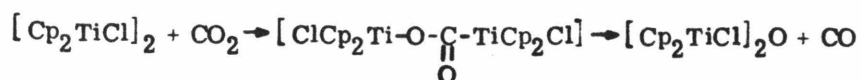


Figure 9

When the osmium tetraoxide-Vaska's complex reaction is carried out without pyridine, the carbon monoxide ligand is not oxidized as evidenced by $\nu(\text{C}\equiv\text{O})$ of the product at 2010 cm^{-1} . Analytical material was not isolated, so the formulation of this compound is unclear. Several possibilities derived from osmium tetraoxide chemistry which are compatible with the amorphous black material's infrared spectrum are pictured below (Figure 10). The alkene and quinuclidine analogues have been structurally characterized.¹⁵ The Lewis acid-base complex **A** would be related to the first intermediate in the Sharpless mechanism for alkene oxidation in which the alkene initially reacts with osmium tetraoxide as a weak nucleophile. A strong absorption in the infrared spectrum at 970 cm^{-1} , presumably $\nu(\text{Os}=\text{O})$, is evidence for the second alternative, **B**. The quinuclidine-osmium tetraoxide adduct, similar to **A**, displays three stretches between 900 and 950 cm^{-1} , while the mono-oxo osmium(VI) compounds in olefin chemistry, similar to **B**, have a strong osmium-oxo stretch at 980 cm^{-1} .^{1,16} The first possibility, **A**, is exciting, as it would correspond to a proposed intermediate in alkene oxidation. The second

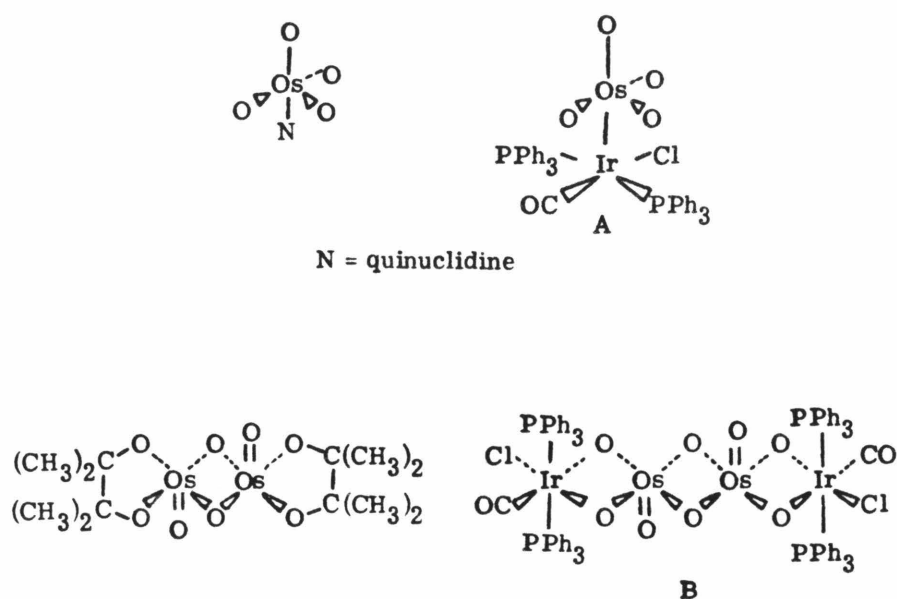
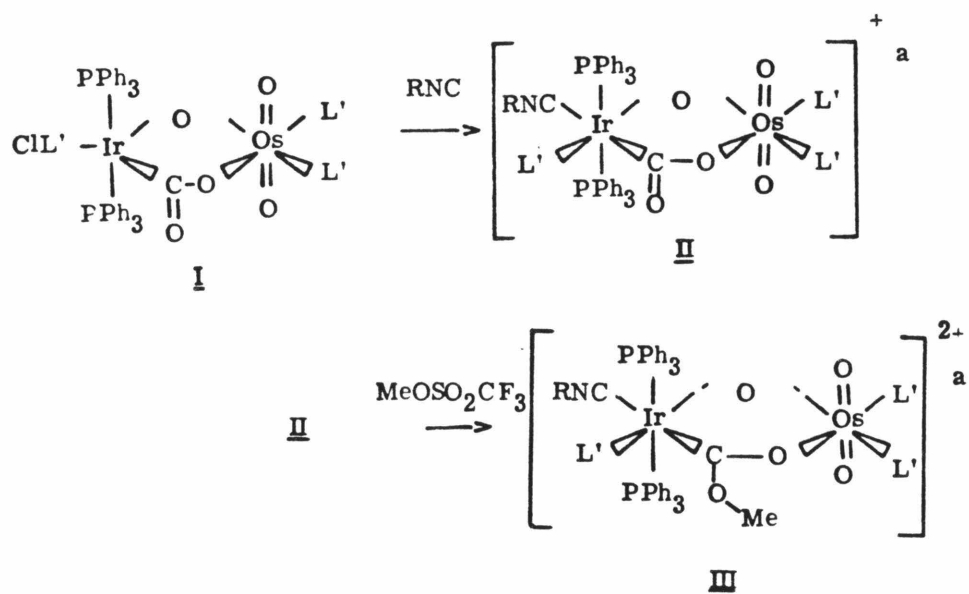


Figure 10

formulation, **B**, seems more reasonable based on the infrared spectrum. The presence of pyridine in the reaction mixture may serve to promote attack on carbon monoxide by providing a ligand for iridium. However, the addition of pyridine to this black material does not result in formation of the bridging carbon dioxide complex. Unfortunately, this amorphous black material could not be cleanly isolated.

The formulation of compound **I** as a unique bridging carbon dioxide complex made a crystal structure very desirable. Structural crystals could not be obtained, so derivatization of **I** was undertaken. Reaction with tert-butyl isocyanide results in displacement of chloride, giving compound **II**, isolated as a perchlorate salt. Finally, reaction of **II**, with excess methyl



L' = 4-tert-butylpyridine

R = tert-butyl

^a Isolated and characterized as the perchlorate salt.

Figure 11

trifluoromethanesulfonate yields the carbene **III**, also isolated as the perchlorate salt (Figure 11). Structural crystals of **III** could be isolated.

The infrared spectra of **II** and **III** demonstrate the presence of tert-butyl isocyanide ($\nu(\text{NC})$ at 2180 cm^{-1} in **II**, and 2200 cm^{-1} in **III**) with the trans-dioxo osmium(VI) fragment still intact. In compound **II**, the bridging carbon dioxide fragment is unperturbed, while in **III**, methylation has considerably reduced the carbonyl bond order ($\nu(\text{C-O})$ at 1255 cm^{-1}). ^{13}C and ^{31}P NMR spectra show equivalent phosphines on iridium for both compounds. The ^{13}C NMR bridging carbon dioxide resonance shifts further downfield from its position in compound **I** with each derivatization reaction. This chemical shift phenomenon can partially be attributed to the increased cationic deshielding with each derivatization step.¹⁷ The increased cationic character is also reflected in the appearance of $\nu(\text{NC})$ for the tert-butyl isocyanide ligand. The $\nu(\text{NC})$ band is shifted from 2180 cm^{-1} in **II** to 2200 cm^{-1} in compound **III**. This results from decreased π -backbonding in the dication relative to the cation.

The geometry at iridium in compound **II** is completely defined by the structural determination of compound **III** (Figure 12). The isocyanide ligand is trans to the carbene ligand while the pyridine ligand is trans to the bridging oxo ligand. The osmium coordination environment is quite similar to diolatodioxobis(amine)osmium(VI) ester structures. In both, the oxo-osmium-oxo angle is not linear, but bent away from the diolato oxygens toward the pyridine ligands. This angle in compound **III** is $161.2(4)^\circ$ compared to $164.0(5)^\circ$ for diolatodioxobis(amine)osmium(VI) ester compounds. This departure from linearity is due to π -interactions of the oxo ligands with the

bridging oxygen atoms.¹⁸

Careful examination of the bond lengths of the carbene portion suggest that the carbene might be better described as a bridging ester. The ester carbonyl bond length of 1.338(16) Å appears shorter than the C-OMe bond length, 1.418(16) Å. There is a degree of uncertainty in this comparison because of the standard deviations of the bond lengths. The carbonyl oxygen of this ester resonance structure serves as a Lewis base to osmium (Figure 13).

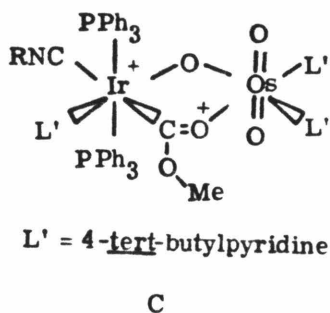


Figure 13

This resonance structure C spreads the dicationic charge throughout the molecule.

In Fischer-type carbene complexes, isomers such as **D** and **E** result from hindered rotation about the C-OMe bond (Figure 14). The methyl resonance in compound **III**, which appears at 3.5 δ in the ¹H NMR spectrum is temperature independent from 40°C to -70°C. This suggests either the presence of only one of the two possible carbene isomers in solution or free

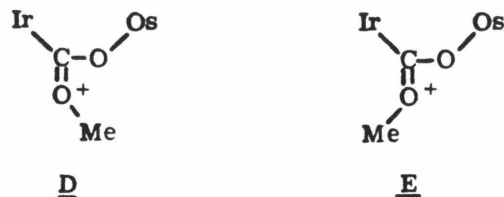


Figure 14

rotation about the C-OMe bond. The free rotation could result from the predominant bridging ester resonance structure. The carbene ^{13}C NMR resonance generally shifts much further downfield upon methylation to form the carbene than is observed with compound **III**.¹⁷ The small downfield shift to 221 ppm is due to the fact that the bridging ester resonance structure reduces the positive charge on the carbene carbon. In Fischer-type carbenes, such as pentacarbonyl(methoxy(phenyl)carbene)chromium(0), the carbene carbon is very positively charged. The observed chemical shift of 351.4 ppm lies within the range of carbocations in organic chemistry.¹⁷ Some of the cationic character of compound **III** is dispersed to the osmium center as demonstrated by a 20 cm^{-1} shift to higher energy of the trans-dioxo asymmetric stretch upon methylation. The stronger osmium-oxo bond in the dicationic complex appears borne out in the crystal structure. The average osmium oxygen distance is $1.720(8)\text{ \AA}$ while in the analogous diolato-dioxo-bis(amine)osmium(VI) ester complexes, the osmium-oxygen distance is 1.74 \AA .¹⁵ This comparison is not absolute because of the standard deviations of these bond lengths. The structure also demonstrates a distinction between the two osmium pyridine ligands. One pyridine is co-planar with the iridium-

carbene-osmium plane and the corresponding osmium-N3 distance is 0.1 Å longer than the osmium-N2 distance in which the pyridine (N2) is roughly perpendicular to the aforementioned plane. The dihedral angle formed by the two pyridines is 97(3)°. This bond length difference results from crystal packing forces and/or a large degree of π -bonding in the osmium-pyridine (N2) bond.

An interesting feature related to the osmium pyridines is the observation of temperature dependence in the ^1H NMR spectra for compounds **I** and **II** (Figure 15). This temperature dependence is attributed to pyridine lability at osmium. Between 1 and 2 δ , signals appear for the tert-butyl protons of the pyridines and isocyanide ligand in compound **II**. At 2°C, signals appear at 1.45 and 1.23 δ . As the temperature is raised, coalescence is reached at 50°C, and a single resonance appears at 1.34 δ for the two osmium 4-tert-butylpyridines. A resonance at 1.14 δ appears at all temperatures as does a resonance at 1.23 δ coincident with the fluxional 1.23 δ resonance. These are assigned to the tert-butyl protons of the isocyanide and pyridine ligands on iridium. The two fluxional signals are attributed to the tert-butyl signals of the osmium pyridine ligands. This is consistent with lability of osmium(VI) compounds and inertness of iridium(III) compounds. If pyridine is added to the sample, it is readily substituted onto osmium as the high temperature signal at 1.34 δ disappears and a signal for uncoordinated 4-tert-butylpyridine appears in the ^1H NMR spectrum.

The process consistent with this NMR behavior involves dissociation of a 4-tert-butylpyridine ligand giving a five-coordinate osmium(VI) intermediate. The dissociated 4-tert-butylpyridine can then coordinate to the

osmium resulting in equivalence of the two osmium 4-tert-butylpyridine ligands (path a, Figure 16).

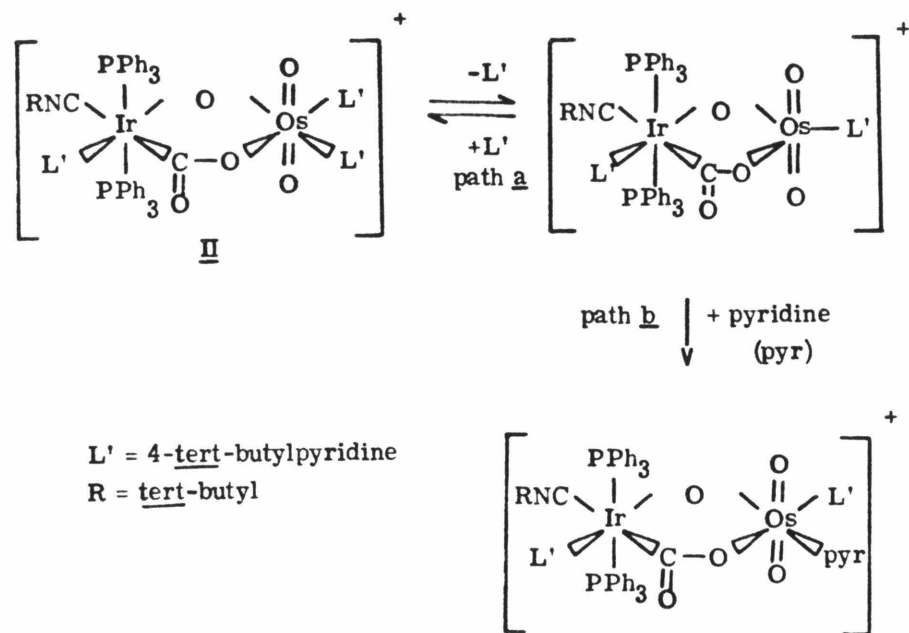


Figure 16

If excess pyridine is present, a pyridine can coordinate resulting in loss of 4-tert-butylpyridine (path b, Figure 16). There is ample precedent for this process as an analogue of the five-coordinate intermediate has been made in alkene chemistry by using a sterically hindered amine, quinuclidine (Figure 17).^{16,19} In chloroform, it is primarily monomeric, but for structural analysis, only dimeric crystals were isolated. The structure of the dimer shows that

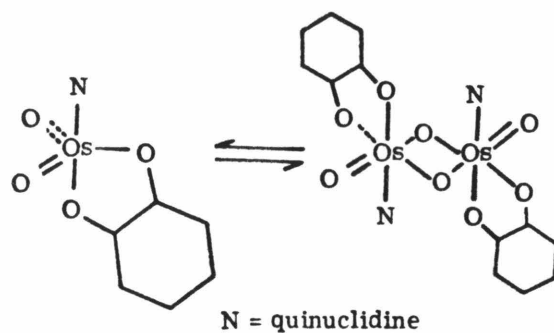


Figure 17

the bridging oxo ligands are not equally disposed between the two osmium centers.

This reactivity of osmium tetroxide is quite analogous to the reactions of osmium tetroxide with alkenes. In addition to carbon monoxide oxidation, attempts were made to generate similar bridging, dinuclear compounds from the nitrosyl and thiocarbonyl analogues of Vaska's complex (Figure 18).

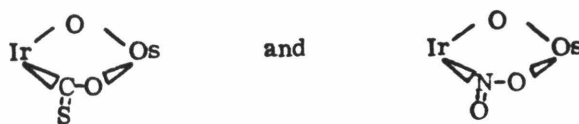


Figure 18

Although these reactions appear promising, characterizable material could not be obtained. In choosing other substrates to generate dinuclear complexes

with osmium tetroxide, it is important that the substrates not contain oxidizable ligands which readily dissociate. Substrates must also be unreactive with pyridine relative to osmium tetroxide. The substrates should also readily undergo two-electron oxidation reactions similar to Vaska's complex. An attempt at similar reactivity using ruthenium tetroxide and Vaska's complex gave uncharacterizable materials. It is noteworthy that in organic oxidation chemistry, intermediates with ruthenium tetroxide are not isolated. The inability to isolate an intermediate in organic oxidation chemistry parallels the inability to synthesize a ruthenium tetroxide-Vaska's complex adduct.

Structural Analysis

A well-formed crystal from a dichloromethane-ethanol solution roughly 0.3 mm on a side was mounted on a glass fiber with epoxy. Oscillation photographs indicated that the space group was of the triclinic class. The intensity data were collected with MoK α radiation ($\lambda = 0.710688 \text{ \AA}$) and a graphite monochromator.

Unit cell parameters were obtained by least squares refinement of the orientation matrix using 15 centered reflections in the range $23.0^\circ < 2\theta < 29.0^\circ$: $a = 21.10(2) \text{ \AA}$, $b = 12.80(2) \text{ \AA}$, $c = 14.47(2) \text{ \AA}$, $\alpha = 85.78(9)^\circ$, $\beta = 94.04(9)^\circ$ and $\gamma = 94.4(9)^\circ$. The unit cell volume was 3896 \AA^3 . The space group was assigned to P1 since $Z = 2$.

A total of 11393 intensity measurements were recorded for reflections in one hemisphere ($4.0^\circ < 2\theta < 45.0^\circ$) using $0-2\theta$ scans at a constant scan speed of 2° per min with a fixed scan width of 0.85° and 0.90° in 2θ above and below the center point. Background measurements were recorded for approximately 30 sec before and after each scan. The integrated intensities were calculated in the following manner: 3 check reflections were remeasured after every 97 reflections. A linear least squares fit of the intensities of these three reflections implied negligible decay over the 278 h of data collection. Absorption corrections were deemed unnecessary. Observational variances were based on counting statistics plus a term $(0.02 C)$ where C is the scan count. After deletion of systematic absences and averaging of multiple and symmetry-related reflections, the total number of unique data was 10222 of which 6349 were greater than 3σ .

Structure Determination and Refinement. The atomic positions of the

osmium and iridium atoms were derived from the Patterson map. Subsequent Fourier and difference maps revealed the non-hydrogen atoms. Atomic scattering factors were taken from Stewart, Davidson, and Simpson for H, and the "International Tables for X-ray Crystallography" for all others.^{20,21}

Several cycles of full matrix least-squares refinement on all non-hydrogen parameters (including two ethanol molecules of solvation) yielded $R = 11.8\%$ and $G.O.F. = 2.95$ where the number of parameters equalled 567. Hydrogen atoms were placed a distance 0.98 \AA from their respective carbon atom by examining general plane sections of the difference map for methyl hydrogens or by assuming ideal geometry, and were not refined. The final cycle of least-squares refinement gave values for R and $R(3\sigma)$ of 8.6% and 5.5% ; the $G.O.F.$ was 1.66 , and the data-to-parameter ratio was 11.47 . The final values for the atomic parameters are given in Tables 1, 2, and 3.

The following diagram indicates atom notation and connectivity:

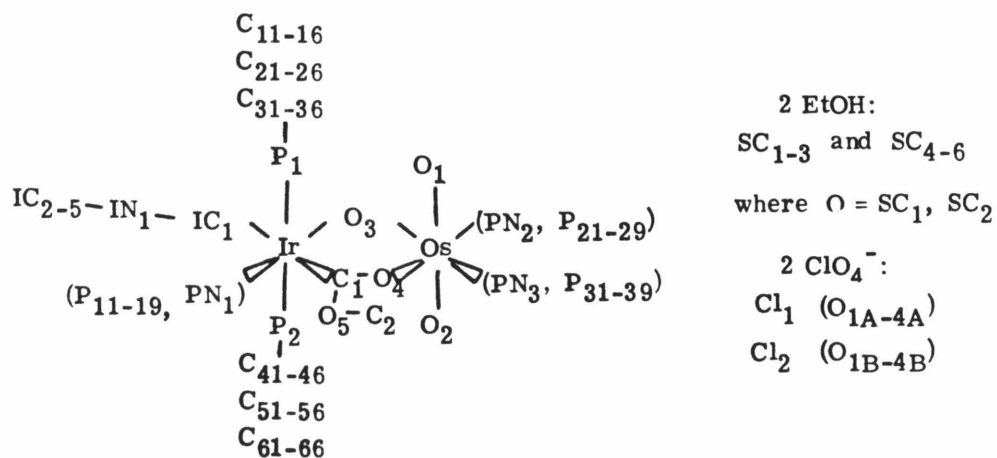


Table 1. Atom Coordinates ($\times 10^5$)

	x	y	z
IR	74511(2)	3823(4)	79553(3)
OS	66717(3)	-16222(4)	68394(4)
P1	79072(17)	-8318(25)	91173(24)
P2	70525(17)	16998(26)	68280(25)
C11	73189(61)	-16424(98)	97566(89)
C12	69513(71)	-11938(107)	103706(104)
C13	64901(79)	-18125(135)	108179(107)
C14	63855(79)	-28773(138)	106656(123)
C15	67635(86)	-32994(126)	100701(119)
C16	72224(65)	-26567(100)	96257(100)
C21	84262(58)	-17555(87)	87316(98)
C22	84326(64)	-19540(98)	78047(99)
C23	88450(75)	-27024(116)	75872(112)
C24	92151(69)	-32197(104)	82777(131)
C25	92188(65)	-30150(104)	91811(110)
C26	88073(70)	-23035(108)	94178(98)
C31	84404(62)	-1174(101)	99264(90)
C32	90071(66)	3080(102)	96369(94)
C33	94304(66)	8749(110)	101623(116)
C34	92998(89)	10383(117)	110613(118)
C35	87401(88)	6270(135)	113865(106)
C36	83188(70)	557(116)	108300(106)
C41	73747(69)	17543(97)	56869(86)
C42	74969(76)	8544(115)	52741(97)
C43	76667(102)	9036(128)	43693(107)
C44	77668(115)	18509(137)	38805(114)
C45	76376(122)	27202(141)	42676(124)
C46	74547(103)	26899(121)	51471(112)
C51	62093(72)	15957(100)	65716(113)
C52	59290(79)	14349(113)	56696(123)
C53	52971(125)	12891(158)	55036(173)
C54	49420(105)	13138(166)	62159(228)
C55	51463(90)	14802(158)	71146(183)
C56	58174(74)	16388(116)	72643(135)
C61	72721(69)	30205(96)	72104(88)
C62	68626(73)	36684(120)	75279(105)
C63	70757(97)	46586(109)	78171(119)
C64	76543(96)	50137(104)	77812(106)
C65	80858(77)	44137(115)	74506(116)
C66	78968(71)	34166(100)	71683(105)
O1	61647(42)	-8864(64)	60413(57)
O2	68878(41)	-26638(61)	75270(56)
O3	73548(38)	-7261(62)	69584(50)
O4	62796(35)	-9628(57)	79161(51)
C1	66253(77)	-1284(96)	82267(92)

Table 1. Continued

O5	62573(37)	1731(59)	89265(58)
C2	56229(65)	-2825(106)	91119(95)
PN1	76410(48)	15441(64)	89400(61)
P11	72509(64)	17831(101)	95620(97)
P12	74026(64)	25107(99)	102151(85)
P13	79713(65)	30789(86)	102174(86)
P14	83592(58)	28398(100)	95844(87)
P15	82060(60)	20995(87)	89657(89)
P16	81303(75)	39393(105)	108905(97)
P17	86958(163)	37364(219)	114212(222)
P18	82245(144)	49558(136)	103830(140)
P19	76608(147)	40082(214)	115212(179)
PN2	70227(45)	-21637(72)	57039(65)
P21	74693(69)	-29114(99)	58144(93)
P22	78026(68)	-31533(103)	50936(101)
P23	77190(65)	-26538(103)	42166(91)
P24	72473(73)	-19791(107)	40769(89)
P25	69213(66)	-17535(95)	48251(89)
P26	81533(72)	-28621(117)	34499(98)
P27	82997(97)	-39667(150)	34883(131)
P28	86870(114)	-21526(195)	35476(175)
P29	78473(123)	-25695(201)	24997(134)
PN3	57729(48)	-27439(82)	67275(71)
P31	52087(68)	-23829(115)	67467(112)
P32	46746(78)	-30816(127)	66664(118)
P33	46939(63)	-41773(112)	65656(104)
P34	52876(82)	-44370(110)	65587(131)
P35	58168(72)	-37634(112)	66500(131)
P36	41189(78)	-49279(135)	64349(152)
P37	36372(121)	-47011(195)	71056(231)
P38	42339(118)	-59721(175)	65680(273)
P39	37846(134)	-47440(264)	55562(221)
CL1	63867(28)	7734(46)	22126(42)
O1A	60018(94)	6162(147)	14261(158)
O2A	70031(88)	4811(166)	21736(170)
O3A	64907(89)	18613(143)	22703(130)
O4A	61698(132)	4515(255)	29798(166)
CL2	99477(71)	35388(34)	81490(30)
O1B	94699(69)	27731(122)	79801(112)
O2B	105123(21)	30970(156)	83803(107)
O3B	99975(113)	41181(143)	73043(121)
O4B	98045(66)	41622(109)	88799(97)
IC1	83221(56)	6509(80)	74272(86)
IN1	87430(46)	6893(75)	69951(68)
IC2	93001(67)	6434(114)	64375(100)

Table 1. Continued

IC3	91091(83)	-2754(130)	58205(114)
IC4	98390(69)	3833(143)	71175(174)
IC5	93796(75)	16787(118)	58860(110)
HC32	9111(0)	194(0)	9003(0)
HC33	9830(0)	1169(0)	9913(0)
HC34	9606(0)	1446(0)	11456(0)
HC35	8641(0)	743(0)	12020(0)
HC36	7920(0)	-239(0)	11077(0)
HC42	7465(0)	174(0)	5633(0)
HC43	7716(0)	255(0)	4072(0)
HC44	7929(0)	1891(0)	3258(0)
HC45	7678(0)	3398(0)	3904(0)
HC46	7378(0)	3349(0)	5411(0)
HC52	6206(0)	1435(0)	5152(0)
HC53	5104(0)	1159(0)	4881(0)
HC54	4486(0)	1206(0)	6089(0)
HC55	4855(0)	1490(0)	7613(0)
HC56	6000(0)	1788(0)	7889(0)
HC62	6412(0)	3434(0)	7554(0)
HC63	6772(0)	5101(0)	8052(0)
HC64	7789(0)	5709(0)	7992(0)
HC65	8528(0)	4691(0)	7414(0)
HC66	8208(0)	2989(0)	6936(0)
HP11	6827(0)	1415(0)	9555(0)
HP12	7101(0)	2619(0)	10676(0)
HP14	8777(0)	3219(0)	9567(0)
HP15	8515(0)	1959(0)	8523(0)
HP21	7548(0)	-3274(0)	6428(0)
HP22	8108(0)	-3694(0)	5200(0)
HP24	7140(0)	-1657(0)	3456(0)
HP25	6591(0)	-1256(0)	4708(0)
HP31	5166(0)	-1635(0)	6812(0)
HP32	4258(0)	-2804(0)	6681(0)
HP34	5351(0)	-5176(0)	6485(0)
HP35	6237(0)	-4036(0)	6665(0)
HM1	5296(0)	146(0)	8812(0)
HM2	5560(0)	-999(0)	8914(0)
HM3	5572(0)	-322(0)	9803(0)
HM11	8644(0)	3066(0)	11897(0)
HM12	8906(0)	4275(0)	11845(0)
HM13	9062(0)	3531(0)	11060(0)
HM14	8662(0)	5359(0)	10565(0)
HM15	7911(0)	5460(0)	10481(0)
HM16	8240(0)	4895(0)	9707(0)
HM17	7620(0)	4777(0)	11697(0)
HM18	7222(0)	3847(0)	11184(0)

Table 1. Continued

HM19	7681(0)	3581(0)	12084(0)
HM21	7982(0)	-4421(0)	3823(0)
HM22	8721(0)	-4040(0)	3874(0)
HM23	8352(0)	-4231(0)	2889(0)
HM24	9041(0)	-2602(0)	4006(0)
HM25	8654(0)	-1568(0)	3899(0)
HM26	8937(0)	-1987(0)	3009(0)
HM27	8114(0)	-2088(0)	2077(0)
HM28	7721(0)	-3209(0)	2109(0)
HM29	7433(0)	-2222(0)	2505(0)
HM31	3519(0)	-3991(0)	7074(0)
HM32	3742(0)	-5192(0)	7174(0)
HM33	3839(0)	-4834(0)	7798(0)
HM34	3930(0)	-6486(0)	6933(0)
HM35	4665(0)	-6084(0)	6982(0)
HM36	4311(0)	-6370(0)	6009(0)
HM37	4014(0)	-4180(0)	5179(0)
HM38	3689(0)	-5353(0)	5190(0)
HM39	3348(0)	-4450(0)	5630(0)
HM11	8754(0)	-111(0)	5365(0)
HM12	9469(0)	-450(0)	5461(0)
HM13	8974(0)	-928(0)	6196(0)
HM14	9726(0)	-239(0)	7563(0)
HM15	9984(0)	973(0)	7511(0)
HM16	10224(0)	191(0)	6817(0)
HM17	9826(0)	1976(0)	5945(0)
HM18	9109(0)	2187(0)	6111(0)
HM19	9263(0)	1607(0)	5217(0)

Table 1. Continued

SC1	10434(12)	4020(18)	4267(17)
SC1	9731(18)	3809(28)	4075(24)
SC3	9588(13)	2701(22)	3547(19)
SC4	5485(10)	2652(17)	9652(14)
SC5	5714(20)	3669(32)	9934(29)
SC6	5211(19)	3516(30)	10760(27)
HC12	7022(0)	-446(0)	10479(0)
HC13	6234(0)	-1500(0)	11248(0)
HC14	6051(0)	-3313(0)	10979(0)
HC15	6696(0)	-4048(0)	9965(0)
HC16	7485(0)	-3023(0)	9213(0)
HC22	8165(0)	-1590(0)	7323(0)
HC23	8869(0)	-2860(0)	6939(0)
HC24	9487(0)	-3752(0)	8102(0)
HC25	9503(0)	-3359(0)	9652(0)
HC26	8780(0)	-2178(0)	10074(0)

Table 2. Bond Distances $\overset{\circ}{\text{Å}}$

IR-P1	2.407(3)	C53-C54	1.322(35)
IR-P2	2.417(3)	C54-C55	1.368(34)
IR-O3	2.086(8)	C55-C56	1.425(28)
IR-C1	1.869(14)	C61-C62	1.369(20)
IR-PN1	2.132(11)	C61-C66	1.385(19)
IR-IC1	2.043(11)	C62-C63	1.396(23)
OS-O1	1.726(8)	C63-C64	1.298(24)
OS-O2	1.711(8)	C64-C65	1.371(23)
OS-O3	1.866(8)	C65-C66	1.390(21)
OS-O4	2.029(7)	PN1-P11	1.331(16)
OS-PN2	2.088(9)	PN1-P15	1.345(15)
OS-PN3	2.215(10)	P11-P12	1.380(18)
C1-O4	2.138(11)	P12-P13	1.359(18)
C1-O5	1.418(16)	P13-P14	1.340(18)
O5-C2	1.461(16)	P13-P16	1.526(19)
P1-C11	1.819(13)	P14-P15	1.357(18)
P1-C21	1.817(13)	P16-P17	1.408(35)
P1-C31	1.816(13)	P16-P18	1.453(27)
P2-C41	1.826(14)	P16-P19	1.409(32)
P2-C51	1.797(15)	PN2-P21	1.390(17)
P2-C61	1.833(14)	PN2-P25	1.349(16)
C11-C12	1.403(19)	P21-P22	1.367(20)
C11-C16	1.375(14)	P22-P23	1.384(19)
C12-C13	1.377(22)	P23-P24	1.366(19)
C13-C14	1.394(17)	P23-P26	1.541(20)
C14-C15	1.382(25)	P24-P25	1.384(19)
C15-C16	1.362(22)	P26-P27	1.467(25)
C21-C22	1.384(18)	P26-P28	1.401(29)
C21-C26	1.415(19)	P26-P29	1.512(28)
C22-C23	1.412(21)	PN3-P31	1.318(18)
C23-C24	1.387(22)	PN3-P35	1.329(19)
C24-C25	1.351(21)	P31-P32	1.392(23)
C25-C26	1.385(20)	P32-P33	1.425(22)
C31-C32	1.361(19)	P33-P34	1.327(22)
C31-C36	1.387(20)	P33-P36	1.503(23)
C32-C33	1.340(20)	P34-P35	1.366(23)
C33-C34	1.383(23)	P36-P37	1.515(34)
C34-C35	1.361(24)	P36-P38	1.374(34)
C41-C42	1.385(20)	P36-P39	1.424(36)
C41-C46	1.387(22)	CL1-O1A	1.371(21)
C42-C43	1.378(23)	CL1-O2A	1.393(20)
C43-C44	1.368(26)	CL1-O3A	1.401(29)
C44-C45	1.337(28)	CL1-O4A	1.261(29)
C45-C46	1.353(27)	CL2-O1B	1.376(16)
C51-C52	1.418(22)	CL2-O2B	1.373(17)

Table 2. Continued

C51-C56	1.353(22)	CL2-O3B	1.388(20)
C52-C53	1.345(29)	CL2-O4B	1.433(15)
IN1-IC2	1.483(17)	IC1-IN1	1.121(15)
IC2-IC3	1.541(22)	S1-S2	1.503(43)
IC2-IC4	1.495(22)	S2-S3	1.657(45)
IC2-IC5	1.500(21)	S4-S5	1.431(47)
		S5-S6	1.648(57)

Table 3. Angles

P1-IR-P2	175.7(1)	C1-O5-C2	125.1(9)
P1-IR-O3	92.6(2)	IR-P1-C11	113.4(4)
P1-IR-C1	91.7(4)	IR-P1-C21	117.3(4)
P1-IR-PN1	86.8(3)	IR-P1-C31	109.7(4)
P1-IR-IC1	88.6(3)	C11-P1-C21	104.8(6)
P2-IR-O3	90.6(2)	C11-P1-C31	109.4(6)
P2-IR-C1	91.5(4)	C21-P1-C31	101.4(6)
P2-IR-PN1	89.8(3)	IR-P2-C41	115.7(4)
P2-IR-IC1	89.0(3)	IR-P2-C51	115.4(5)
O3-IR-C1	84.5(3)	IR-P2-C61	110.6(7)
O3-IR-PN1	174.5(3)	C41-P2-C51	103.7(7)
O3-IR-IC1	81.1(4)	C41-P2-C61	102.8(6)
C1-IR-PN1	100.9(5)	C51-P2-C61	107.6(7)
C1-IR-IC1	165.6(5)	O1A-CL1-O2A	114.6(12)
PN1-IR-IC1	93.5(4)	O1A-CL1-O3A	106.9(12)
O1-OS-O2	161.2(4)	O1A-CL1-O4A	117.3(16)
O1-OS-O3	100.7(3)	O2A-CL1-O3A	101.4(12)
O1-OS-O4	91.7(4)	O2A-CL1-O4A	110.5(16)
O1-OS-PN2	86.7(4)	O3A-CL1-O4A	104.1(15)
O1-OS-PN3	81.7(4)	O1B-CL2-O2B	110.6(10)
O2-OS-O3	97.5(3)	O1B-CL2-O3B	104.5(11)
O2-OS-O4	93.2(4)	O1B-CL2-O4B	111.2(9)
O2-OS-PN2	90.0(4)	O2B-CL2-O3B	108.2(11)
O2-OS-PN3	80.0(4)	O2B-CL2-O4B	109.4(9)
O3-OS-O4	89.2(3)	O3B-CL2-O4B	112.8(10)
O3-OS-PN2	86.0(3)	IC1-IN1-IC2	175.2(12)
O3-OS-PN3	177.5(3)	IN1-IC2-IC3	103.7(11)

Table 3. Continued

O4-OS-PN2	174.5(3)	IN1-IC2-IC4	105.9(12)
O4-OS-PN3	91.4(4)	IN1-IC2-IC5	106.9(11)
PN2-OS-PN3	93.5(4)	IC3-IC2-IC4	110.8(13)
IR-O3-O5	120.6(4)	IC3-IC2-IC5	112.6(13)
IR-C1-O4	129.4(10)	IC4-IC2-IC5	115.8(13)
IR-C1-O5	128.1(9)	S1-S2-D3	109.6(25)
O4-C1-O5	101.7(10)	S4-S5-S6	88.3(27)
OS-O4-C1	115.4(7)		
	X = 1	5	3
P1-CX1-CX2	120.4(10)	121.6(10)	118.7(10)
P1-CX1-CX6	120.2(10)	117.7(10)	125.6(10)
CX2-CX1-CX6	119.4(12)	120.7(12)	115.7(12)
CX1-CX2-CX3	119.5(13)	116.7(12)	124.0(13)
CX2-CX3-CX4	120.8(15)	121.0(14)	119.3(14)
CX3-CX4-CX5	118.4(14)	122.5(15)	119.0(15)
CX4-CX5-CX6	122.0(15)	117.7(14)	120.1(16)
CX5-CX6-CX1	119.8(12)	121.2(13)	121.8(14)
	X = 4	5	6
P2-CX1-CX2	121.9(10)	122.7(11)	125.1(11)
P2-CX1-CX6	121.8(11)	119.5(12)	118.5(10)
CX2-CX1-CX6	116.0(13)	117.7(14)	116.3(13)
CX1-CX2-CX3	120.9(14)	121.8(17)	121.0(14)
CX2-CX3-CX4	120.7(16)	117.4(22)	122.1(16)
CX3-CX4-CX5	118.5(18)	127.0(24)	119.8(16)
CX4-CX5-CX6	121.7(19)	114.1(20)	120.1(15)
CX5-CX6-CX1	121.9(17)	121.9(16)	120.6(13)
	X = 1	2	3
M*-PNX-PX1	126.5(8)	121.8(8)	118.7(9)
M*-PNX-PX5	119.1(7)	123.4(8)	122.2(9)
PX1-PNX-PX5	114.7(10)	114.6(10)	119.3(12)
PNX-PX1-PX2	124.4(12)	121.9(12)	118.8(14)
PX1-PX2-PX3	119.9(12)	121.6(13)	124.3(15)
PX2-PX3-PX4	115.2(12)	117.2(13)	110.9(14)
PX2-PX3-PX6	120.7(12)	120.0(12)	124.6(14)
PX4-PX3-PX6	124.0(12)	122.8(12)	124.5(15)
PX3-PX4-PX5	123.8(12)	119.1(13)	125.6(16)
PX4-PX5-PNX	121.9(11)	125.1(12)	121.2(15)
PX3-PX6-PX7	109.4(16)	111.9(13)	108.7(17)
PX3-PX6-PX8	110.4(14)	106.2(15)	114.8(18)
PX3-PX6-PX9	113.6(16)	110.7(14)	112.4(18)
PX7-PX6-PX8	108.2(18)	114.2(16)	108.3(20)
PX7-PX6-PX9	107.0(20)	108.7(15)	102.3(20)
PX8-PX6-PX9	108.1(17)	105.0(16)	109.4(21)

*M = IR (X = 1) or OS (X = 2, 3)

Experimental Section

Preparation of I, The Bridging Carbon Dioxide Complex. Osmium tetroxide (260 mg) was dissolved in a toluene solution containing 2.0 mL of tert-butylpyridine. The solution was cooled to -40°C , and trans-carbonylchlorobis(triphenylphosphine)iridium(I) (780 mg) was added. The yellow solution was allowed to warm, and the color became orange-brown. The solution was stirred at room temperature for 10 min, and the addition of hexane precipitated a light brown solid. This powder was dissolved in dichloromethane-butyl ether with several drops of tert-butylpyridine. The dichloromethane was removed on the rotary evaporator and an orange-brown solid separated overnight (900 mg, 62%). The ^1H NMR spectrum showed di-n-butyl ether as a solvate.

Anal. calcd. for $\text{C}_{64}\text{H}_{69}\text{ClIr}_3\text{N}_3\text{O}_5\text{P}_2\text{Os}\cdot\frac{1}{3}\text{bu}_2\text{O}$: C, 53.97; H, 5.10; N, 2.83. Found: C, 54.15; H, 5.29; N, 2.80.

Preparation of II, The Bridging Carbon Dioxide Perchlorate Salt. Compound I (400 mg) was dissolved in dichloromethane with excess tert-butyl isocyanide. The mixture was stirred at room temperature for 5 min. Hexane was added and the dichloromethane was removed on the rotary evaporator. The precipitate was dissolved in dichloromethane-ethanol saturated with sodium perchlorate. Removal of the dichloromethane afforded brown crystals (350 mg, 79%). The ^1H NMR spectrum showed water as a solvate.

Anal. calcd. for $\text{C}_{69}\text{H}_{78}\text{ClIr}_3\text{N}_4\text{O}_9\text{P}_2\text{Os}\cdot\text{H}_2\text{O}$: C, 51.63; H, 5.02; N, 3.49. Found: C, 51.49; H, 4.95; N, 3.53.

Preparation of III, The Carbene Perchlorate Salt. Compound II was added to dry benzene. Addition of excess methyl trifluoromethanesulfonate

dissolved the starting material, and compound **III** precipitated. This material was dissolved in dichloromethane-ethanol saturated with sodium perchlorate. Removal of dichloromethane afforded brown crystals (180 mg, 84%). The ^1H NMR spectrum showed water and dichloromethane as solvates.

Anal. calcd. for $\text{C}_{70}\text{H}_{81}\text{Cl}_2\text{N}_4\text{O}_{13}\text{P}_2\text{IrOs}\cdot\frac{1}{4}\text{CH}_2\text{Cl}_2\cdot\frac{5}{4}\text{H}_2\text{O}$: C, 48.34; H, 4.85; N, 3.21. Found: C, 48.33; H, 4.81; N, 3.21.

Reaction of Osmium Tetraoxide With Trans-carbonylchlorobis(triphenylphosphine)iridium(I). Trans-carbonylchlorobis(triphenylphosphine)iridium(I) (100 mg) was added to a benzene solution of osmium tetraoxide (60 mg). The solution immediately turned black, and stirring was continued for 15 min. Upon addition of hexane, a black powder was precipitated. It was filtered and washed with hexane. The yield was 100 mg.

Table 4. Relevant Infrared Data (cm⁻¹).

compound	$\nu_{\text{C=O}}$	$\nu_{\text{C-O}}$	ν_{OsO_2}	$\nu_{\text{N}\equiv\text{C}}$
I	1593	1022	820	
I- ¹³ C	1560	1010	820	
I- ¹⁸ O	1592	1010	780	
II	1583	a	823	2180
II- ¹³ C	1555	a	823	2180
II- ¹⁸ O	1583	a	785	2180
compound	CO ₂ Me	ν_{OsO_2}	$\nu_{\text{N}\equiv\text{C}}$	
III	1255	840	2200	
III- ¹³ C	1230	840	2200	
III- ¹⁸ O	1255	800	2200	
	$\nu_{\text{C}\equiv\text{O}}$	ν_{OsO}		
Vaska's Complex + OsO ₄	2010	980		

^a-Obscured by ClO₄⁻ bands.

Table 5. ^{31}P and ^{13}C NMR Data (δ ppm)

Compound	δ $^{31}\text{P}^{\text{b}}$	δ $^{13}\text{C}^{\text{c}}$	$^2\text{J}^{13}\text{C}-^{31}\text{P}$ (Hz) $^{\text{d}}$
I	-14.0	187.2	7.0
II	-18.2	207.5	8.8
III	-19.2	221.1	8.8

^a Jeol FX 90Q, solvent CDCl_3 . ^b Relative to external standard H_3PO_4 . ^c Relative to internal standard TMS. ^d Obtained from ^{13}C and ^{31}P spectra.

Table 6. ^1H NMR Data (CDCl_3).

Compound	Chemical Shift (δ) and Coupling Constants				
$\text{I} \cdot \frac{1}{3}$ butyl ether	compound	1.15	s	9H	
		1.30	s	9H	
		1.40	s	9H	
		6.9-8.4	m	42H	
	solvate	0.8-1.8	m	4H	
		3.4	t	2H	6=J(HH)
$\text{II} \cdot \text{H}_2\text{O}$	compound	0.9	s	9H	
		1.3 and 1.5	s	27H	
		6.6-8.3	m	42H	
	solvate	1.8	s	2H	
$\text{III} \cdot \frac{1}{4} \text{CH}_2\text{Cl}_2 \cdot 1\frac{1}{4} \text{H}_2\text{O}$	compound	1.15	s	9H	
		1.3	s	9H	
		1.4	s	9H	
		1.5	s	9H	
		3.5	s	3H	
		6.8-8.6	m	42H	
	solvate	1.7	s	$2\frac{1}{2}\text{H}$	
	5.3	s	$\frac{1}{2}\text{H}$		

References and Notes

- (1) Schroder, M. Chem. Rev. **1980**, 80, 187.
- (2) Dewar, M. J. S. Ind. Chim. Belge. **1950**, 15, 181.
- (3) Dewar, M. J. S.; Longuet-Higgins, H. C. Proc. R. Soc., London, Ser. A **1952**, 214, 482.
- (4) Dewar, M. J. S. J. Am. Chem. Soc. **1952**, 74, 3341.
- (5) Sharpless, K. B.; Teranishi, A. Y.; Backvall, J. E. J. Am. Chem. Soc. **1977**, 99, 3120.
- (6) Collin, R. J.; Jones, J.; Griffith, W. P. J. Chem. Soc., Dalton Trans. **1974**, 1094.
- (7) Cotton, F. A.; Wilkinson, G. "Advanced Inorganic Chemistry"; Interscience Publishers: New York, 1972; p. 153.
- (8) Wilkinson, G.; Stone, F. G. A.; Abel, E. W. "Comprehensive Organometallic Chemistry"; Pergamon Press: New York, 1982; Vol. 8, p. 225.
- (9) Aresta, M.; Nobile, C. F.; Albano, V. G.; Forni, E.; Manassero, M. J. Chem. Soc., Chem. Commun. **1975**, 636.
- (10) Bristow, G. S.; Hitchcock, P. B.; Lappert, M. F. J. Chem. Soc., Chem. Commun. **1981**, 1145.
- (11) Herskovitz, T.; Guggenberger, L. J. J. Am. Chem. Soc. **1976**, 98, 1615.
- (12) Guy, J. J.; Sheldrick, G. M. Acta Cryst. **1978**, B-34, 1718.
- (13) Fachinetti, G.; Floriani, C.; Chiesi-Villa, A.; Guastini, C. J. Am. Chem. Soc. **1978**, 100, 7405.
- (14) Fachinetti, G.; Floriani, C.; Chiesi-Villa, A.; Guastini, C. J. Am.

Chem. Soc. **1979**, 101, 1767.

- (15) (a) Phillips, F. L.; Skapski, A. C. J. Chem. Soc., Dalton Trans. **1975**, 2586. (b) Collin, R. J.; Griffith, W. P.; Phillips, F. L.; Skapski, A. C. Biochim. Biophys. Acta **1973**, 320, 745. (c) Griffith, W. P.; Skapski, A. C.; Woods, K. A.; Wright, M. J. Inorg. Chim. Acta **1978**, L413.
- (16) Cleave, M. J.; Hydes, P. C.; Griffith, W. P.; Wright, M. J. J. Chem. Soc., Dalton Trans. **1977**, 941.
- (17) (a) Kreiter, C. G.; Formacek, V. Angew. Chem. **1972**, 84, 155. (b) Fischer, E. O. Nobel Lecture, The Nobel Foundation, 1974.
- (18) Kistenmacher, T. J.; Marzilli, L. G.; Rossi, M. Bioinorg. Chem. **1976**, 6, 347.
- (19) Cartwright, B. A.; Griffith, W. P.; Schroder, M.; Skapski, A. C. J. Chem. Soc., Chem. Commun. **1978**, 853.
- (20) Stewart, R. F.; Davidson, E. R.; Simpson, W. T. J. Chem. Phys. **1965**, 42, 3157.
- (21) "International Tables for X-ray Crystallography"; Kynoch Press: Birmingham, England, 1974; p. 155.

CHAPTER III

Peroxy-carboxylic Acid

Introduction

The reactions of peroxy-carboxylic acids with low valent organo-metallic complexes such as Vaska's complex have been studied not only to identify the products but also to understand the reaction mechanism. An initial hope of the study was the possible isolation of a 1,3-dipolar adduct (Figure 1).

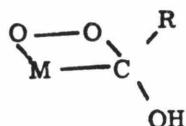


Figure 1

The peroxy-carboxylic acid's behavior as a 1,3-dipole has been suggested in olefin epoxidation, but this behavior has not been absolutely demonstrated (Figure 2).¹

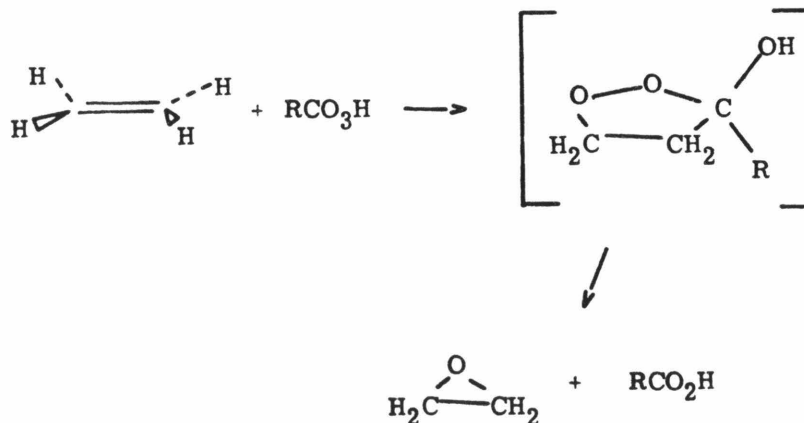


Figure 2

The Bartlett mechanism in which an electrophilic oxygen of the peroxy-carboxylic acid is transferred to the olefin is widely preferred (Figure 3).²

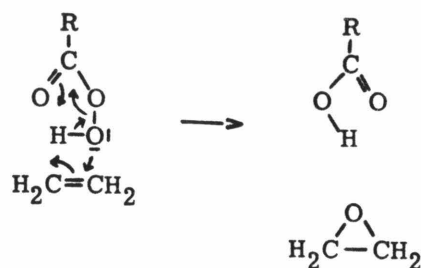


Figure 3

The possibility of synthesizing a 1,3-dipolar peracid adduct on a metal center seems reasonable since similar adducts have been proposed as intermediates for the reactions of organic azides with organometallic complexes (Figure 4).³

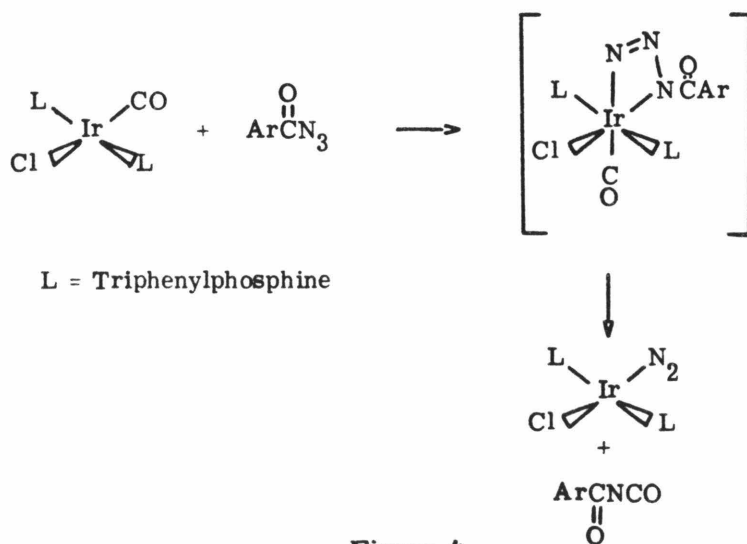


Figure 4

Tetracyanoethylene oxide's reaction with $\text{Pt}(\text{AsPh}_3)_2$ gives a structurally characterized 1,3-dipolar adduct (Figure 5).⁴

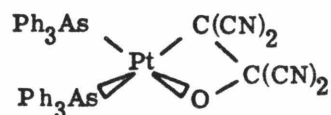


Figure 5

The existence of peroxymetallacycles in the reactions of electrophiles with coordinated dioxygen in $\text{Pt}(\text{PPh}_3)_2\text{O}_2$ lends additional support for the isolation of a 1,3-dipolar peracid adduct (Figure 6).⁵

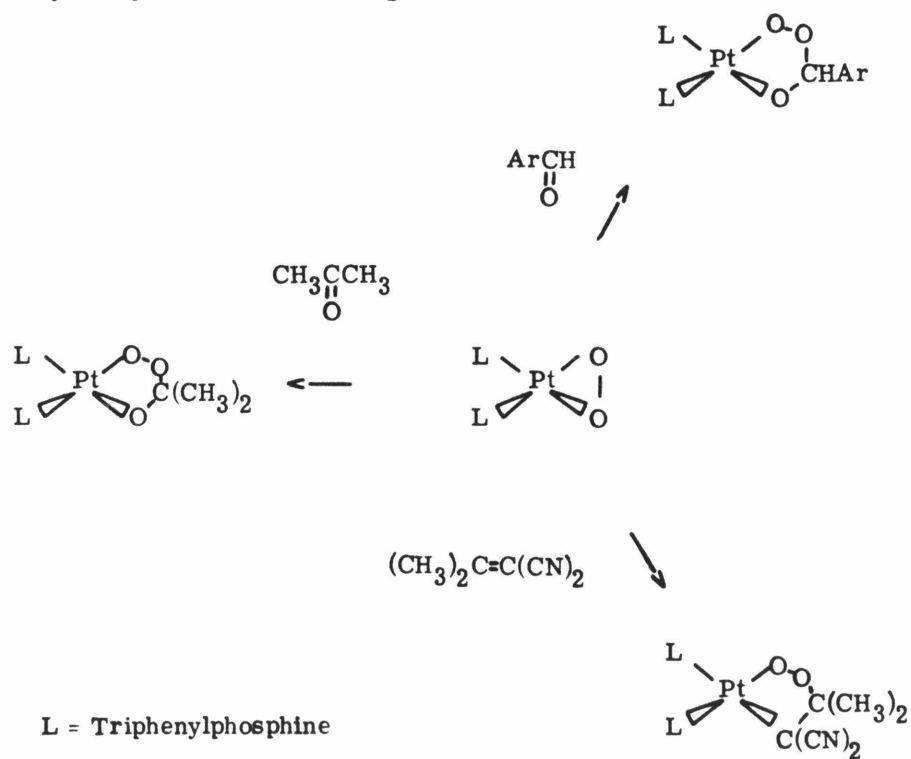


Figure 6

Finally, an aryl nitrile N-oxide which reacts with several organic substrates as a 1,3-dipole, readily gives a 1,3-dipolar adduct with an anionic rhodium complex (Figure 7).⁶

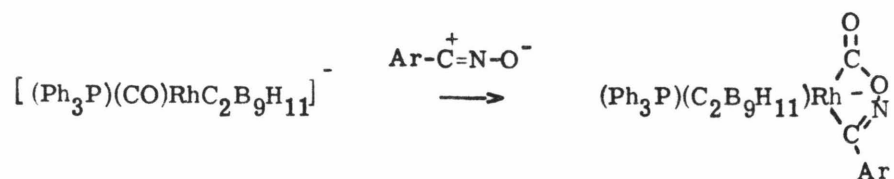


Figure 7

As this work progressed, it became obvious that the desired 1,3-dipolar adduct could not be synthesized. Instead, the metal center and carbon monoxide ligand were oxidized. During this work, an article appeared in which this reaction and several speculative mechanisms were discussed.⁷ Some of our additional independent results suggest that a better mechanism should be considered.

There are several reasonable modes of reactivity that can be envisioned for the reaction of a peroxy-carboxylic acid with Vaska's complex due to the number of reactive bonds in the peroxy-carboxylic acid molecule. Oxidative addition can occur utilizing (1) the O-O bond, or (2) the O-H bond in addition to the previously discussed (3) 1,3-dipolar adduct (Figure 8).

To complicate this question, the products indicated in reactions (1), (2), and (3) can undergo further reactions. If the reaction progresses with retention of the O-O bond, as in reactions (2) and (3), subsequent rearrangement could result in the oxidation of ligands such as carbon monoxide and triphenylphosphine to carbon dioxide and triphenylphosphine

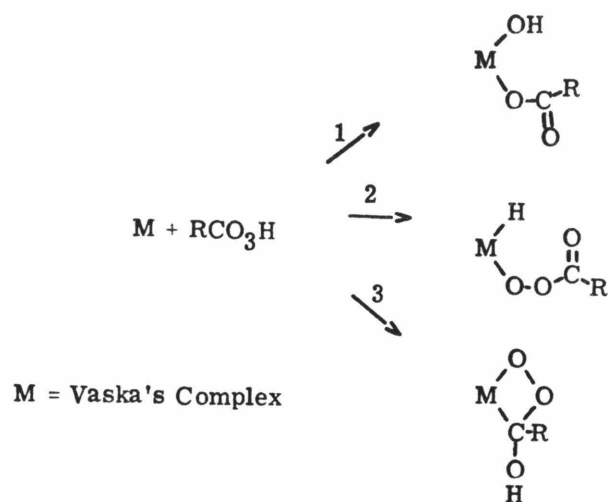


Figure 8

oxide. Even the product observed in reaction (1) is subject to further reactivity. The monodentate carboxylate could become bidentate, eliminating hydroxide to generate the cationic complex (Figure 9).

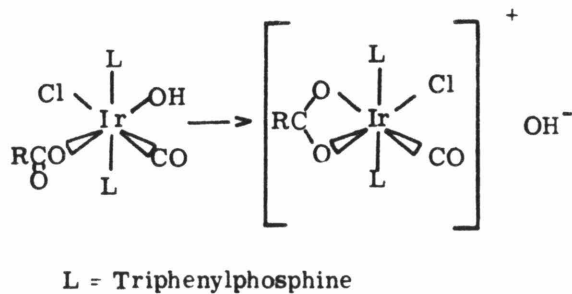


Figure 9

This cationic complex may be initially formed in the interaction of the peroxy-carboxylic acid with iridium(I) starting material. The cationic complex could subsequently undergo nucleophilic attack at the carbon monoxide ligand by hydroxide or by a peroxy-carboxylate anion, either of which could extrude carbon dioxide (Figure 10).

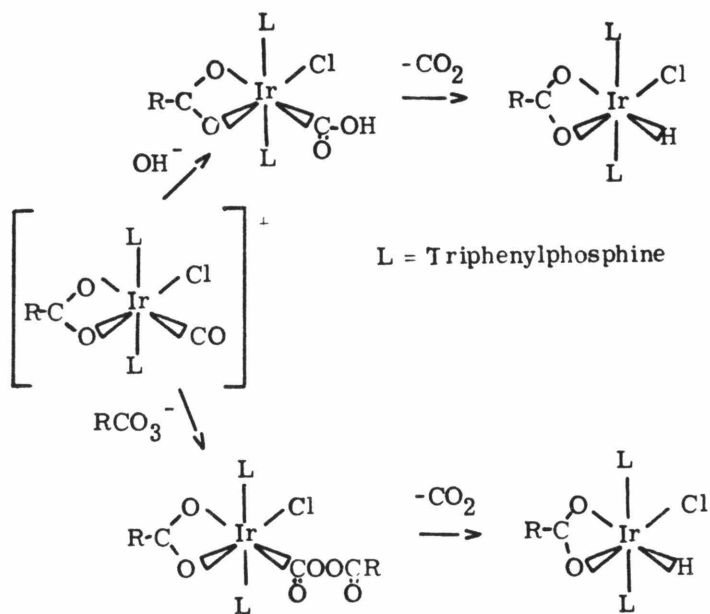


Figure 10

The peroxy-carboxylate anion could easily be generated from hydroxide and the peroxy-carboxylic acid.

Electron transfer from the electron rich transition metal complex to the peroxy-carboxylic acid cannot be discluded as a possibility. Such a process

could result in the product shown in reaction 1 (Figure 8). It has been observed that the reactivities of peroxy compounds with low valent transition metal complexes parallels the ease of reduction of the peroxy compounds.⁵ Whether this indicates that an electron-transfer mechanism is operative, or simply that the more potent oxidant is more reactive via another mechanism is uncertain.

A variety of products from reactions of peroxy compounds with transition metal complexes have been synthesized.⁷⁻¹⁴ These reactions were investigated because it was suggested that the autoxidation of olefins was a free radical process initiated by the transition metal complex and traces of peroxy contaminants in the alkene substrate.¹⁵⁻²² Since radical pathways occur in these systems, clean chemistry is seldom obtained. The reactions of diacyl peroxides, alkyl hydroperoxides, and peroxycarboxylic acids with d^8 and d^{10} transition metal complexes have yielded fairly clean results.⁷⁻¹⁴ In iridium chemistry, only the reaction of alkyl hydroperoxides with Vaska's complex indicated free radical processes. It was the purpose of our work to attain a mechanistic understanding for the reaction of a peroxycarboxylic acid with Vaska's complex in addition to product identification. Our sequence of reactions suggests a mechanism different from several proposed in the literature.⁷

Results

The O-O bond is not retained in any of the iridium compounds derived from peroxycarboxylic acids. Infrared spectroscopy has proven very useful in

demonstrating the bonding mode of the resultant carboxylato ligand.²³ In this series of compounds, the carboxylato ligand is either monodentate or bidentate. For a bidentate carboxylato ligand, ν_a (CO₂) and ν_s (CO₂) have a very narrow separation. They appear at approximately 1490 cm⁻¹ and 1420 cm⁻¹, respectively. For a monodentate carboxylato ligand, this separation is much larger as ν_a (CO₂) appears at around 1650 cm⁻¹ and ν_s (CO₂) appears at 1330 cm⁻¹.

The reaction of the peroxy-carboxylic acid with Vaska's complex requires at least two equivalents to consume all of the iridium(I) starting material. In the process, the carbon monoxide ligand is oxidized to carbon dioxide. This is confirmed by using carbon-13 labeled carbon monoxide in the starting material. The final product has two carboxylato ligands. The infrared spectrum demonstrates that one is bidentate and the other is monodentate. At what stage of the reaction is the carbon monoxide oxidized?

A publication appeared describing this reaction while our work was being completed.⁷ Bird, et. al., also successfully characterized the final product, and proposed several mechanisms for its formation (Figure 11). Although both of their mechanisms arrive at the same iridium hydride intermediate, the initial steps differ. Oxidative addition of the O-H bond is proposed in **I**, while O-O bond cleavage is conjectured in **II**. When the reaction is carried out in the presence of an external acid such as tetrafluoroboric acid, the cation in **II** is isolated as the tetrafluoroborate salt. This suggests that the initial interaction of the peroxy-carboxylic acid with Vaska's complex results in O-O bond cleavage as shown in **II**. The formation

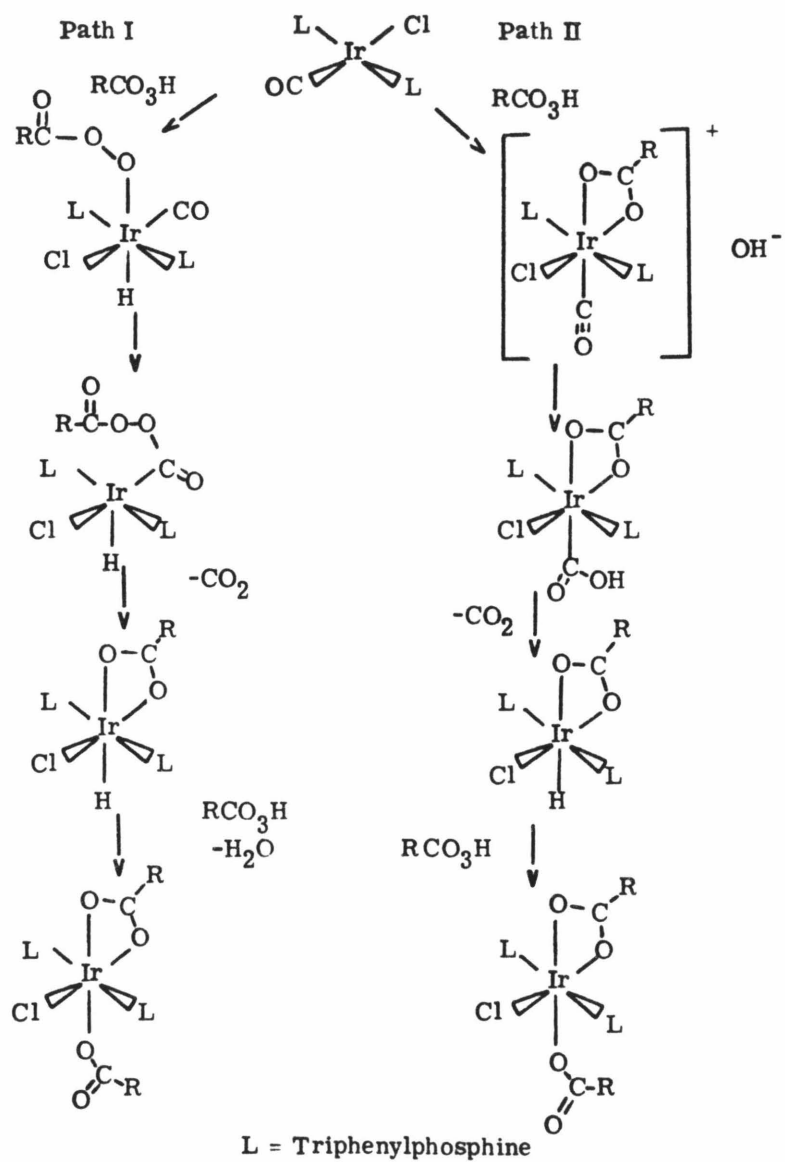


Figure 11

of this cation will be discussed later. A key feature of both mechanisms is the last step where the proposed iridium hydride reacts with the peracid to generate the observed product. The iridium hydride complex was independently synthesized and its reaction with the peroxy-carboxylic acid does not yield any of the desired product as pictured in these two mechanisms. Instead, an uncharacterizable blue-green material is obtained.

How does the transformation of the iridium cation to the final product proceed? We propose that instead of hydroxide attacking the carbon monoxide as a nucleophile (II), the hydroxide is scavenged by another equivalent of the peroxy-carboxylic acid, and the resultant peroxy-carboxylate anion rather than hydroxide attacks the carbon monoxide ligand of the cationic complex. Our alternative mechanism is pictured below (Figure 12).

If the reaction is carried out in the presence of excess tetrafluoroboric acid, the reaction is intercepted before the carbon monoxide is oxidized. An explanation is that the tetrafluoroboric acid neutralizes the hydroxide before the second equivalent of peroxy-carboxylic acid can be deprotonated. Without tetrafluoroboric acid, the resulting peroxy-carboxylate nucleophile could attack the carbon monoxide, followed by extrusion of carbon dioxide giving the observed product. One can generate the peroxy-carboxylate anion from peroxy-carboxylic acid and tetraethylammonium hydroxide. When the iridium cation is added to the solution, evolution of carbon dioxide occurs and the final product of the two-equivalent peroxy-carboxylic acid reaction is generated in 60% yield.

Critical to this mechanistic suggestion is the fact that the peroxy-carboxylic acid itself is incapable of oxidizing the carbon monoxide of

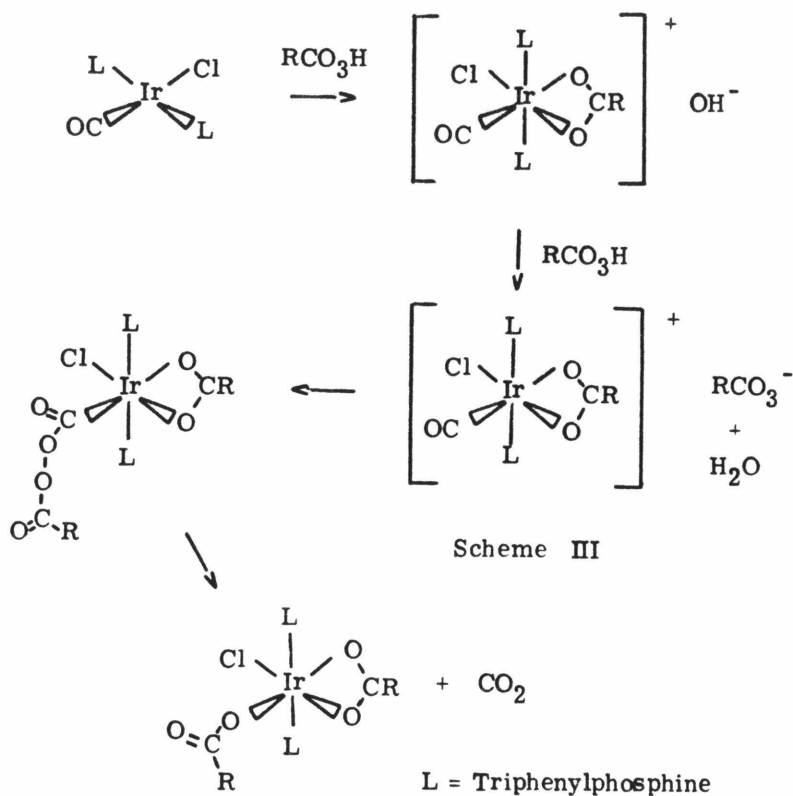


Figure 12

the iridium(III) tetrafluoroborate salt. It is necessary to generate the peroxycarboxylate anion in order to observe the oxidation to carbon dioxide. This reaction sequence is interesting in that the peroxycarboxylic acid reacts in two fashions. Initially, O-O bond cleavage is observed. This is followed by the peroxycarboxylic acid behaving as a Brønsted acid with the resulting anion reacting as a nucleophile.

The attack of nucleophiles at carbon monoxide in cationic transition metal compounds is well documented.²⁴ In addition to attack of the

peroxycarboxylate anion, we have shown that other nucleophiles are capable of demonstrating similar reactivity with the iridium(III) cation. The reaction of hydroxide itself with the cation results in loss of the carbon monoxide stretch in the infrared spectrum and the generation of an uncharacterizable green material. Ethoxide and ammonia react with the cation to generate ethoxycarbonyl and metalcarbamoyl compounds. These reactions are reversible. For instance, the addition of tetrafluoroboric acid to the ethoxycarbonyl liberates ethanol and regenerates the iridium salt. Similarly, the addition of methyl trifluoromethanesulfonate generates methyl ethyl ether and the iridium cation (Figure 13).

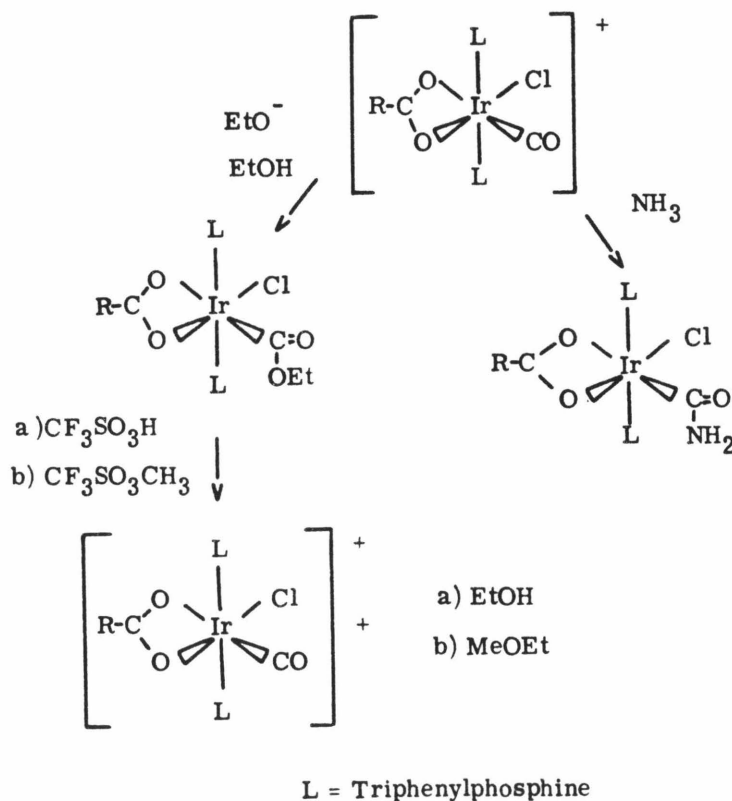


Figure 13

We propose that the actual intermediate prior to the loss of carbon dioxide is pictured in Figure 14. There is precedent for this proposed intermediate in the osmium tetroxide chemistry described in Chapter II. The product of the osmium tetroxide reaction retains the carbon dioxide ligand and is readily isolated. Loss of carbon dioxide readily occurs from the proposed peroxy-carboxylate intermediate. This facile extrusion of carbon dioxide can be rationalized by the availability of a coordination site in the intermediate via a bidentate-to-monodentate carboxylato ligand conversion.

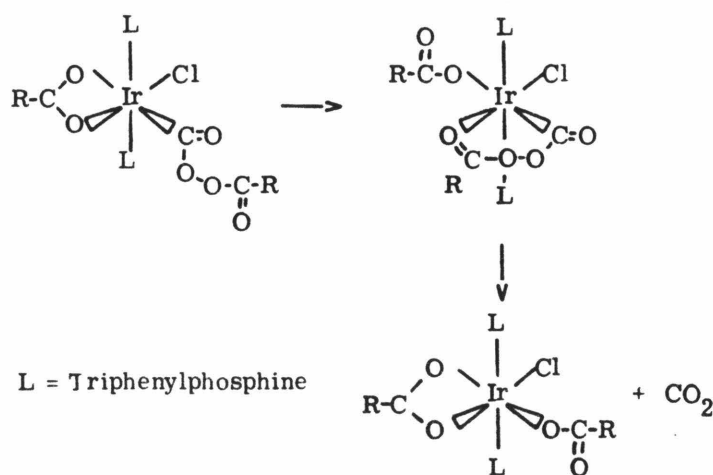


Figure 14

A number of reactions demonstrate the bidentate-monodentate coordinative dexterity of the carboxylato ligand. Acetonitrile readily coordinates to the iridium center of the cationic iridium(III)tetrafluoroborate. Tert-butyl isocyanide coordinates to iridium in the ethoxycarbonyl complex

giving a monodentate carboxylate. The reaction of iodide with the cation results in complete removal of the carboxylato ligand and uptake of two equivalents of iodide.

At the outset of this work, it was hoped that the initial peroxycarboxylic acid interaction with the iridium complex could be determined. The exact nature of the intermediate after the initial equivalent of peracid reacts with Vaska's complex remains questionable. It appears that O-O bond cleavage results. The resulting hydroxide could be bound to the metal, or it may be a counterion. Attempts to synthesize an iridium(III) hydroxide analogous to the proposed intermediate have been unsuccessful. The deprotonation of the peroxycarboxylic acid with tetraethylammonium hydroxide and the subsequent reaction with the carbonyl cation suggest that the hydroxide is not bound to the metal. However, it is not unreasonable to assume that the peroxycarboxylic acid could protonate a metal bound hydroxide. Water then dissociates with the carboxylato ligand becoming bidentate, and the peroxycarboxylate anion could then oxidize the carbon monoxide.

Not only is it uncertain whether the hydroxide is bound to the metal, it is also unclear what processes may proceed O-O bond cleavage. The O-O bond cleavage could result from an electron-transfer mechanism (Figure 15).

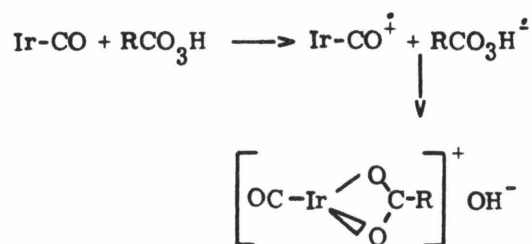


Figure 15

A 1,3-dipolar adduct may form initially, and its subsequent decomposition results in formation of the cation (Figure 16).

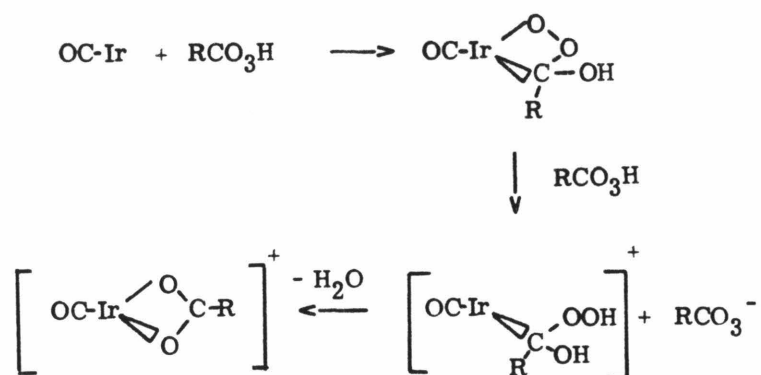


Figure 16

Finally, O-O bond cleavage may result from oxidative addition with subsequent loss of hydroxide facilitated by a monodentate-bidentate carboxylato ligand conversion (Figure 17).

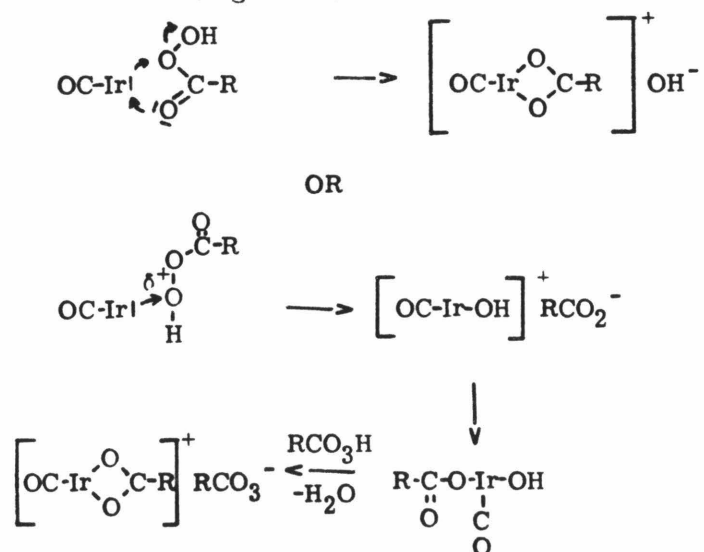


Figure 17

A minor side product observed in the reaction of Vaska's complex with two equivalents of peroxy-carboxylic acid is chlorobis(m-chlorobenzoato)-carbonylbis(triphenylphosphine)iridium(III). The formation of this product can easily be explained by the suggested mechanism. A minor decomposition impurity in peroxy-carboxylic acids is the corresponding carboxylic acid. After the initial equivalent of peroxy-carboxylic acid reacts, the hydroxide can be scavenged by the carboxylic acid and the resulting carboxylate anion can attack the cationic iridium(III) compound giving the observed product. The carboxylic acid present may be the result of peracid decomposition during the course of the reaction. The infrared spectrum of this side product is identical to the product obtained from the reaction of the corresponding diacylperoxide with Vaska's complex. This side product can be obtained in up to 40% yield by varying the conditions of the peroxy-carboxylic acid-tetraethylammonium hydroxide reaction with the iridium cation to allow for decomposition of the peroxy-carboxylate anion prior to reaction with the iridium cation.

The same workers that independently published their peroxy-carboxylic acid results, also noted that the nitrogen analogue of Vaska's complex, trans-chloronitrogenbis(triphenylphosphine)iridium(I) reacts with peroxy-carboxylic acids to give the same product but in significantly poorer yield.⁷ This is readily explained if the initial interaction with the peroxy-carboxylic acid results in O-O bond cleavage, and free hydroxide is generated. Nitrogen would evolve from any iridium(III) compound present. The same product would be observed if the carboxylic acid impurity scavenged the hydroxide, and the resulting carboxylate anion coordinated to the metal. It is noteworthy that a

large amount of phosphine oxide is generated in the reaction of the nitrogen analogue. A by-product of this ligand oxidation would be the hydroxide-scavenging carboxylic acid (Figure 18).

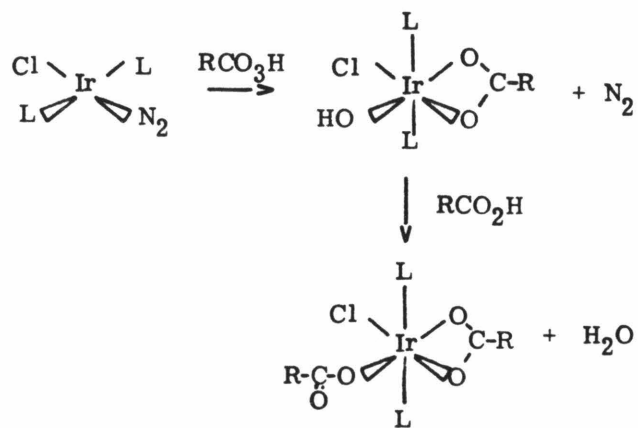


Figure 18

We can duplicate the final product of the peroxycarboxylic acid reaction in two independent steps which makes strong implications about the course of the reaction. It is not obvious what the initial interaction of the peroxycarboxylic acid with the transition metal complex is. From our results, it is apparent that O-O bond cleavage probably occurs. Further work is needed to fully understand the initial reaction of peroxycarboxylic acids with low valent transition metal compounds.

Structural Analysis

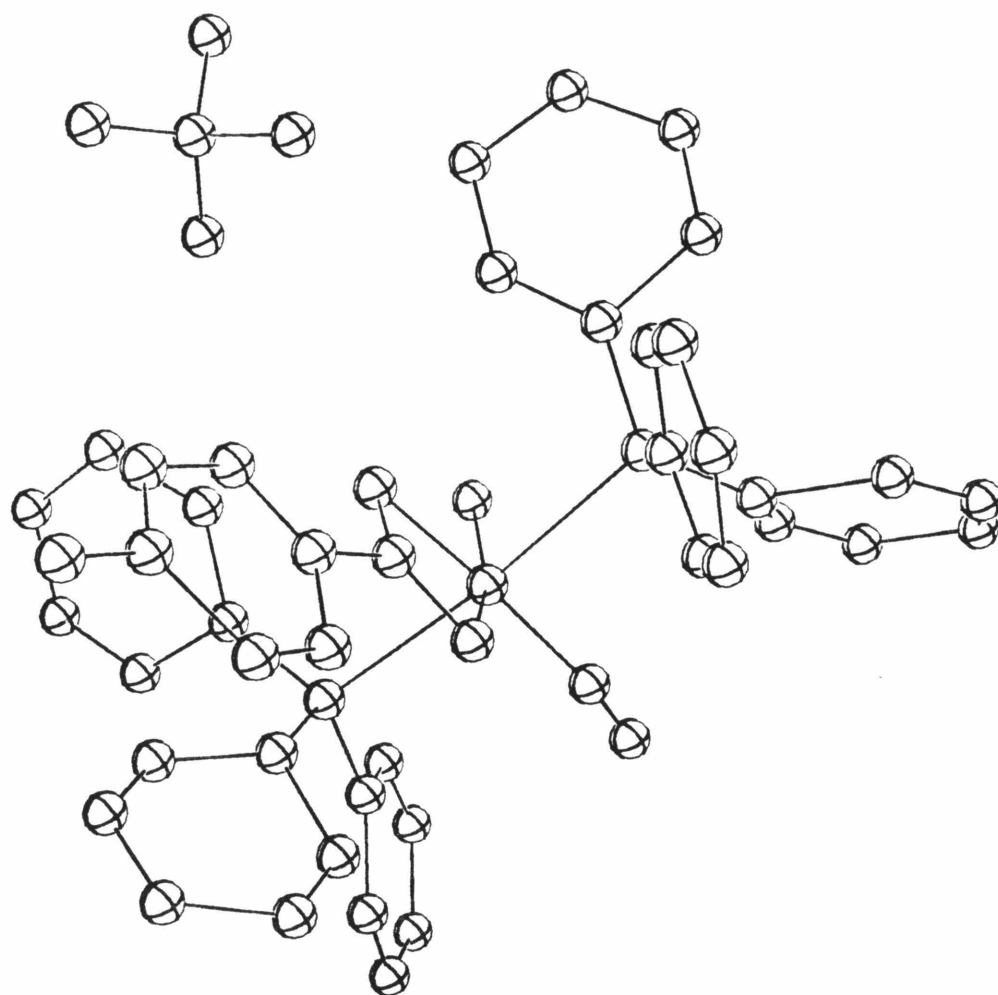
Because of the mechanistic implications of the iridium(III) cation, a structural analysis of it was undertaken. Critical bond distances and angles are given in Tables 1 and 2, and the ORTEP is pictured in Figure 19. The result of this structural investigation is consistent with the spectroscopic data obtained from this compound. The phosphines are located trans and the benzene fragment of the bidentate carboxylato ligand is coplanar with the carboxylato fragment.

The carbon monoxide ligand could not be refined as this ligand was disordered. Because of thermal motion, attempts to refine resulted in the oxygen atom converging with the carbon atom. Because of this difficulty, these atom locations were derived from a Fourier difference map and were not refined.

Data Collection. A crystal of the toluato-cation roughly 0.3 mm on a side was obtained from the slow evaporation of a dichloromethane-cyclohexane solution and mounted on a glass fiber with epoxy. Oscillation photographs indicated that the space group was of the monoclinic class. The intensity data were collected with MoK α radiation ($\lambda = 0.71069 \text{ \AA}$) and a graphite monochromator at 18 $^{\circ}$ K.

Unit cell parameters were obtained by least-squares refinement of the orientation matrix using 15 centered reflections in the range $25^{\circ} < 2\theta < 34^{\circ}$: $a = 12.901(9)$, $b = 21.355(19)$, $c = 14.956(18) \text{ \AA}$, $\alpha = 90^{\circ}$, $\beta = 99.05(7)^{\circ}$, $\gamma = 90^{\circ}$, and $V = 4069(7) \text{ \AA}^3$. The systematic absences lead to the assignment of the space group $P2_1/n$ ($h0l$: $h + 1 = 2n + 1$; $0k0$: $k = 2n + 1$).

A total of 10338 intensity measurements were recorded for reflections



ORTEP of Chloro(p-methylbenzoato)carbonylbis(triphenylphosphine)iridium(III) -
tetrafluoroborate

Figure 19

Table 1. Atomic Distances (Å).

Ir-Cl	2.341 (7)	C22-C23	1.435 (41)
Ir-P1	2.460 (6)	C23-C24	1.466 (40)
Ir-P2	2.470 (6)	C24-C25	1.461 (30)
Ir-O1	2.123 (16)	C25-C26	1.319 (30)
Ir-O2	2.134 (16)	C21-C26	1.307 (32)
Ir-CT1	2.534 (21)	C31-C32	1.358 (29)
P1-C11	1.689 (33)	C32-C33	1.344 (31)
P1-C21	1.787 (23)	C33-C34	1.418 (36)
P1-C31	1.867 (21)	C34-C35	1.389 (39)
P2-C41	1.863 (23)	C35-C36	1.411 (37)
P2-C51	1.871 (24)	C31-C36	1.346 (32)
P2-C61	1.822 (23)	C41-C42	1.375 (39)
O1-O2	2.192 (22)	C42-C43	1.457 (47)
O1-CT1	1.331 (26)	C43-C44	1.603 (44)
O2-CT1	1.284 (26)	C44-C45	1.466 (39)
CT1-CT2	1.399 (35)	C45-C46	1.383 (35)
CT2-CT3	1.495 (38)	C41-C46	1.400 (31)
CT3-CT4	1.322 (35)	C51-C52	1.346 (31)
CT4-CT5	1.414 (38)	C52-C53	1.286 (29)
CT5-CT8	1.357 (37)	C53-C54	1.449 (29)
CT5-CT6	1.355 (40)	C54-C55	1.328 (29)
CT6-CT7	1.462 (40)	C55-C56	1.378 (29)
CT7-CT2	1.354 (41)	C51-C56	1.363 (31)
C11-C12	1.530 (43)	C61-C62	1.429 (35)
C12-C13	1.472 (36)	C62-C63	1.426 (38)
C13-C14	1.388 (31)	C63-C64	1.363 (39)
C14-C15	1.470 (39)	C64-C65	1.511 (40)
C15-C16	1.237 (41)	C65-C66	1.378 (38)
C11-C16	1.580 (41)	C61-C66	1.345 (34)
C21-C22	1.428 (33)		

The following diagram indicates atom notation and connectivity:

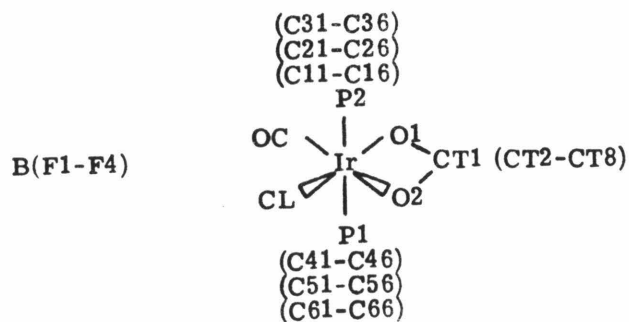


Table 2. Bond Angles (degrees).

P1-Ir-Cl	87.9	(2)	C14-C13-C12	120.7	(21)
P2-Ir-Cl	91.1	(2)	C15-C14-C13	117.3	(22)
O1-Ir-Cl	166.4	(5)	C16-C15-C14	129.4	(29)
O2-Ir-Cl	104.5	(4)	C11-C16-C15	118.0	(26)
P2-Ir-P1	174.7	(2)	C22-C21-P1	117.6	(17)
O1-Ir-P1	90.0	(5)	C26-C21-P1	126.4	(18)
O2-Ir-P1	87.8	(4)	C23-C22-C21	125.3	(23)
O1-Ir-P2	89.8	(5)	C24-C23-C22	111.8	(25)
O2-Ir-P2	87.4	(4)	C25-C24-C23	121.8	(21)
O2-Ir-O1	62.0	(6)	C26-C25-C24	115.4	(19)
C11-P1-Ir	113.3	(11)	C21-C26-C25	129.6	(15)
C21-P1-Ir	104.9	(8)	C32-C31-P1	119.5	(15)
C31-P1-Ir	113.1	(7)	C36-C31-P1	122.3	(16)
C21-P1-C11	109.4	(13)	C33-C32-C31	123.5	(20)
C31-P1-C11	105.9	(13)	C34-C33-C32	118.5	(21)
C31-P1-C21	110.7	(10)	C35-C34-C33	119.7	(24)
C41-P2-Ir	113.3	(7)	C36-C35-C34	117.0	(24)
C51-P2-Ir	115.0	(8)	C31-C36-C35	122.4	(23)
C61-P2-Ir	108.8	(8)	C42-C41-P2	112.7	(19)
C51-P2-C41	107.0	(10)	C46-C41-P2	120.9	(16)
C61-P2-C41	105.9	(10)	C43-C42-C41	117.3	(27)
C61-P2-C51	105.9	(10)	C44-C43-C42	116.4	(27)
CT1-O1-Ir	91.4	(12)	C45-C44-C43	120.2	(24)
CT1-O2-Ir	92.3	(12)	C46-C45-C44	115.3	(23)
O2-CT1-O1	113.9	(18)	C41-C46-C45	124.5	(21)
CT2-CT1-O1	120.2	(20)	C52-C51-P2	120.2	(17)
CT2-CT1-O2	125.8	(21)	C56-C51-P2	119.8	(17)
CT7-CT2-CT1	120.7	(25)	C53-C52-C51	117.3	(20)
CT3-CT2-CT1	117.9	(23)	C54-C53-C52	124.8	(19)
CT2-CT3-CT4	116.5	(23)	C55-C54-C53	118.7	(19)
CT3-CT4-CT5	124.3	(24)	C56-C55-C54	115.3	(19)
CT4-CT5-CT6	115.7	(25)	C51-C56-C55	124.5	(19)
CT5-CT6-CT7	122.3	(26)	C62-C61-P2	118.4	(17)
CT6-CT7-CT2	118.4	(26)	C66-C61-P2	119.5	(18)
CT8-CT5-CT6	124.4	(26)	C63-C62-C61	118.3	(23)
CT8-CT5-CT4	119.8	(25)	C64-C63-C62	121.2	(25)
C12-C11-P1	122.3	(22)	C65-C64-C63	117.2	(25)
C16-C11-P1	122.9	(22)	C66-C65-C64	119.3	(24)
C13-C12-C11	119.1	(24)	C61-C66-C65	120.1	(23)

in one hemisphere ($4.00 < 2\theta < 45.00$) using $0-2\theta$ scans at a constant scan speed of 2.00 per min with a fixed symmetric scan width of 1.00 in 2θ . Background measurements were recorded for approximately 30 sec before and after each scan. The integrated intensities were calculated in the following manner: $I = R (C - T (B_1 + B_2))$ where R is the scan rate, C is the scan count, B_1 and B_2 are the background measurements, and T is the ratio of the scan time to the total background counting time. Four check reflections were remeasured after every 96 reflections. A linear least-squares fit of the intensities of these four reflections implied no decay over the 280 h of data collection. Absorption corrections were deemed unnecessary. Observational variances were based on counting statistics plus a term $0.02 C$ where C is the scan count. After deletion of systematic absences and averaging of multiple and symmetry related reflections, the total number of unique data were 5322 of which 3462 were greater than 3σ .

Structure Determination and Refinement. The atomic positions of the iridium atoms were derived from the Patterson map. Subsequent Fourier and difference maps revealed non-hydrogen atoms. Atomic scattering factors were taken from Stewart, Davidson, and Simpson for H, and the "International Tables for X-ray Crystallography" for all others.^{25,26}

Several cycles of full matrix least squares refinement minimizing $\sum w(F_o^2 - F_c/k)^2$, $w = \sigma^{-2}(F_o)^2$, on all non-hydrogen parameters utilizing all data gave $R = 15.1\%$, $R_{3\sigma} = 12.1\%$, and $G.O.F. = 25.4$.²⁷ Disorder problems and other factors prevented complete refinement of this structure. The carbonyl coordinates were placed in the locations of highest electron density. Refinement in the final stages used only the shell of data

with $2\theta > 26^\circ$ because the low angle data suffered from heavy atom "ripple" effects. The R, $R_{3\sigma}$, and G.O.F. values for the limited data set were 14.7%, 10.8%, and 2.60. The maximum $|\Delta\rho|$ for the limited data set was $3.8 \text{ e}/\text{\AA}^3$. The refinement was stopped at this stage since the structure was adequately determined, and further improvement was not possible.

Table 3

Fractional Atomic Coordinates ($\times 10^5$)

	X		Y		Z		UEQ ($\times 10^4$)	
IR	38707	(7)	6152	(4)	21717	(6)	121	(-3)
CL	47166	(46)	6203	(37)	8933	(39)	295	(14)
P1	22487	(47)	3307	(29)	11772	(41)	178	(40)
P2	54701	(48)	10004	(29)	31213	(42)	193	(16)
B	36751	(450)	35051	(170)	11550	(340)	630	(210)
F1	28425	(100)	38725	(80)	12367	(120)	434	(80)
F2	44362	(115)	37946	(68)	7806	(111)	347	(70)
F3	34091	(116)	29023	(75)	8282	(110)	418	(75)
F4	42106	(120)	34175	(75)	21547	(100)	380	(70)

Fractional Atomic Coordinates ($\times 10^4$)

	X		Y		Z		B (\AA^2)	
O1	2987	(14)	824	(7)	3221	(10)	1.97	(0.30)
O2	3249	(13)	1530	(7)	2226	(10)	1.00	(0.27)
CT1	2772	(17)	1391	(9)	2892	(13)	0.34	(0.35)
CT2	2125	(23)	1788	(13)	3303	(17)	2.49	(0.49)
CT3	1764	(22)	2374	(12)	2821	(17)	1.60	(0.46)
CT4	1159	(20)	2742	(11)	3227	(15)	1.47	(0.42)
CT5	534	(24)	2538	(14)	3870	(18)	2.51	(0.52)
CT6	700	(23)	1946	(12)	4162	(17)	2.09	(0.47)
CT7	1571	(25)	1571	(13)	3937	(19)	2.94	(0.53)
CT8	-216	(19)	2918	(10)	4113	(14)	4.75	(0.40)
C11	2012	(27)	774	(14)	240	(21)	3.60	(0.60)
C12	2442	(23)	1434	(13)	201	(19)	2.36	(0.51)
C13	2044	(18)	1833	(10)	-571	(14)	0.70	(0.36)
C14	1394	(18)	1593	(10)	-1311	(14)	0.87	(0.38)
C15	1090	(26)	937	(15)	-1271	(20)	3.40	(0.55)
C16	1246	(19)	569	(13)	-632	(15)	2.04	(0.41)
C21	1227	(19)	444	(10)	1846	(15)	1.05	(0.41)
C22	388	(21)	851	(11)	1502	(16)	1.53	(0.43)
C23	-550	(27)	944	(15)	1892	(21)	3.53	(0.58)
C24	-538	(16)	586	(12)	2726	(13)	0.84	(0.33)
C25	322	(17)	166	(9)	3057	(13)	0.25	(0.34)
C26	1047	(19)	103	(10)	2528	(14)	1.39	(0.41)
C31	2246	(16)	-489	(9)	774	(13)	0.33	(0.35)
C32	2827	(16)	-647	(12)	125	(13)	1.04	(0.33)
C33	2876	(18)	-1226	(10)	-198	(14)	0.71	(0.38)
C34	2233	(23)	-1690	(13)	108	(18)	2.44	(0.48)
C35	1614	(22)	-1546	(12)	761	(17)	2.66	(0.47)

Table 3. Continued

Fractional Atomic Coordinates ($\times 10^4$)				
	X	Y	Z	B (\AA^2)
C36	1710 (21)	-941 (12)	1127 (16)	1.97 (0.43)
C41	6464 (19)	383 (10)	3451 (15)	1.00 (0.40)
C42	6604 (27)	1 (14)	2744 (20)	3.79 (0.57)
C43	7387 (29)	-488 (15)	2921 (22)	3.64 (0.63)
C44	8079 (23)	-489 (12)	3902 (18)	2.90 (0.51)
C45	7847 (23)	-49 (12)	4592 (18)	2.20 (0.48)
C46	7072 (19)	381 (9)	4306 (14)	0.63 (0.28)
C51	6156 (21)	1649 (10)	2619 (14)	1.19 (0.43)
C52	7202 (17)	1712 (9)	2820 (13)	0.16 (0.34)
C53	7631 (17)	2161 (10)	2442 (13)	0.27 (0.35)
C54	7071 (17)	2570 (10)	1769 (14)	0.38 (0.35)
C55	6038 (17)	2511 (9)	1567 (13)	0.04 (0.34)
C56	5604 (17)	2033 (9)	1999 (13)	0.66 (0.35)
C61	5117 (19)	1301 (11)	4172 (14)	0.83 (0.38)
C62	5314 (21)	1941 (12)	4384 (17)	2.24 (0.46)
C63	5149 (22)	2158 (13)	5250 (18)	2.03 (0.48)
C64	4705 (23)	1788 (13)	5827 (18)	2.55 (0.49)
C65	4365 (24)	1146 (13)	5497 (18)	2.33 (0.51)
C66	4694 (20)	918 (12)	4727 (16)	1.36 (0.42)
C	4190 (0)	-240 (0)	2300 (0)	1.20 (0.00)
O	4380 (0)	-760 (0)	2390 (0)	1.20 (0.00)

Fractional Atomic Coordinates ($\times 10^4$)

H12	2975	1588	684	5.00
H13	2239	2272	-562	5.00
H14	1147	1850	-1839	5.00
H15	709	767	-1831	5.00
H16	904	161	-665	5.00
H22	459	1085	954	5.00
H23	-1129	1214	1634	5.00
H24	-1124	630	3070	5.00
H25	358	-54	3633	5.00
H36	1520	-251	2667	5.00
H32	3233	-321	-121	5.00
H33	3346	-1326	-636	5.00
H34	2227	-2111	-140	5.00
H35	1131	-1849	960	5.00
H36	1375	-847	1656	5.00
H42	6194	55	2144	5.00
H43	7486	-800	2465	5.00
H44	8658	-783	4041	5.00

Table 3. Continued

Fractional Atomic Coordinates ($\times 10^4$)				
	<u>X</u>	<u>Y</u>	<u>Z</u>	<u>B (\AA^2)</u>
H45	8215	-59	5213	5.00
H46	6940	707	4732	5.00
H52	7621	1428	3238	5.00
H53	8383	2230	2620	5.00
H54	7447	2883	1468	5.00
H55	5613	2787	1140	5.00
H56	4847	1965	1851	5.00
H62	5556	2223	3945	5.00
H63	5359	2582	5435	5.00
H64	4611	1931	6430	5.00
H65	3915	895	5827	5.00
H66	4619	475	4584	5.00
HT3	1966	2481	2235	5.00
HT4	1141	3184	3072	5.00
HT6	219	1763	4536	5.00
HT7	1729	1264	4419	5.00

Experimental Section

¹H NMR spectra were obtained with a Varian EM-390 90 MHz spectrometer. Infrared spectra were taken with a Beckman 4240 infrared spectrophotometer. m-Chloroperoxybenzoic acid was purchased from Aldrich and purified by washing with sodium carbonate.

Peroxy Compound Syntheses

Preparation of p-Methylbenzoyl Chloride. p-Methylbenzoic acid (10.0 g) was added to oxalyl chloride (25 mL), and the mixture was refluxed for 12 h. The excess oxalyl chloride was removed. The off-white residue was used without purification for the preparation of p,p'-dimethylbenzoyl peroxide.

Preparation of p,p'-Dimethylbenzoyl Peroxide. p,p'-Dimethylbenzoyl peroxide was prepared in accord with Clarke.²⁸ p-Methylbenzoyl chloride (8.0 g) was dissolved in 50 mL cyclohexane and stirred at 0°C with an excess of aqueous sodium peroxide. The mixture was stirred for 30 min, and the white precipitate was filtered and washed with distilled water and cyclohexane. The crude product was dissolved in benzene, and dried with anhydrous sodium sulfate. It was recrystallized from benzene-cyclohexane. The yield was 4.0 g (57%).

Preparation of p-Methylperoxybenzoic Acid. p-Methylperoxybenzoic acid was prepared according to Organic Syntheses.²⁹ Sodium (0.5 g) was dissolved in 150 mL of dry methanol, and p,p'-dimethylbenzoyl peroxide (5.0 g) was dissolved in 200 mL of dry dichloromethane. Both solutions were cooled to -10°C in a freezing mixture. The peroxide solution was slowly added to the methoxide solution with continuous shaking. Shaking was

continued for 7 min at -10°C after the addition. The reaction was added to a cooled separatory funnel and extracted with a water-ice mixture. The aqueous layer was washed with dichloromethane to remove the methyl benzoate. The *p*-methylperoxybenzoic acid was liberated by acidification with cold 1 N sulfuric acid, and was removed from solution by extraction with dichloromethane. The dichloromethane extracts were combined and dried with anhydrous sodium sulfate. Crystals were obtained with the addition of cyclohexane and removal of dichloromethane (1.5 g, 60%). The purity (95%) was determined by iodometric titration.

Peroxy-carboxylic Acid Reactions

Preparation of Chlorobis(*m*-chlorobenzoato)bis(triphenylphosphine)iridium(III)·Dichloromethane (2:1). A chloroform solution of *m*-chloroperoxybenzoic acid (44 mg) was cooled to -41°C . Trans-chlorocarbonylbis(triphenylphosphine)iridium(I) (100 mg) was added and the solution turned from yellow to golden-brown. The mixture came to room temperature and was washed down a florisil column with dichloromethane. A pink material was obtained which was recrystallized from dichloromethane-ethanol. The yield was 97 mg (68%). The formation of this product was accompanied by evolution of carbon dioxide which was identified by its mass spectrum and infrared spectrum.

Anal. calcd. for $\text{C}_{50}\text{H}_{38}\text{Cl}_3\text{O}_4\text{P}_2\text{Ir}\cdot\frac{1}{2}\text{CH}_2\text{Cl}_2$: C, 54.84; H, 3.53.
Found: C, 54.97; H, 3.63.

Preparation of Chloro(*m*-chlorobenzoato)carbonylbis(triphenylphosphine)iridium(III)tetrafluoroborate. The *m*-chloroperoxybenzoic acid (180

mg) was added to a homogeneous solution of 1 mL tetrafluoroboric acid in benzene and ethanol. Trans-chlorocarbonylbis(triphenylphosphine)iridium(I) (780 mg) was added and slowly dissolved to give a yellow solution. The benzene and ethanol were removed on the rotary evaporator and the remaining material was dissolved in dichloromethane and cyclohexane. This solution was dried with anhydrous sodium sulfate, and the volume was reduced until crystallization began. Pale yellow crystals were obtained in 73% yield (760 mg).

Anal. calcd. for $C_{44}H_{34}BCl_2F_4O_3P_2Ir$: C, 51.67; H, 3.33. Found: C, 51.48; H, 3.47.

Preparation of Chloro(p-methylbenzoato)carbonylbis(triphenylphosphine)iridium(III)tetrafluoroborate. This compound was prepared as described in the previous preparation except 160 mg of p-methylperoxybenzoic acid was substituted for the m-chloroperoxybenzoic acid. By slower evaporation of a dichloromethane-cyclohexane solution of the product, X-ray structural crystals were obtained.

Reactions of Nucleophiles with the Cationic Complex.

Ethoxide. Chloro(p-methylbenzoato)carbonylbis(triphenylphosphine)iridium(III)tetrafluoroborate (100 mg) was added to an ethanolic solution of sodium ethoxide. Dichloromethane was slowly added to dissolve the cation. The solution was stirred for 30 min and the dichloromethane was removed on the rotary evaporator. The yellow solution was set aside until crystallization was complete. A yellow product was obtained in 60% yield (58 mg). Spectroscopic data identified the compound as chloro(ethoxycarboxo)(p-

methylbenzoato)bis(triphenylphosphine)iridium(III).

Anal. calcd. for $C_{47}H_{42}ClO_4P_2Ir$: C, 58.77; H, 4.38. Found: C, 58.50; H, 4.41.

Ammonia. Ammonia was bubbled into a dichloromethane solution of chloro(m-chlorobenzoato)carbonylbis(triphenylphosphine)iridium(III)-tetrafluoroborate (100 mg). Hexane was added to insure the precipitation of all ammonium tetrafluoroborate. The precipitate was filtered and the solvent was evaporated affording a pale yellow solid (66 mg, 70%), identified as (carboxamido)chloro(m-chlorobenzoato)bis(triphenylphosphine)iridium(III).

Anal. calcd. for $C_{44}H_{36}Cl_2NO_3P_2Ir$: C, 55.50; H, 3.80; N, 1.50. Found: C, 54.80; H, 3.91; N, 1.42.

m-Chloroperoxybenzoate. Chloro(m-chlorobenzoato)carbonylbis(triphenylphosphine)iridium(III)tetrafluoroborate (100 mg) and m-chloroperoxybenzoic acid (20 mg) were added to a three-neck flask under a flow of nitrogen. The flask was cooled to $-41^{\circ}C$ and dichloromethane was slowly added. Three drops of 20% tetraethylammonium hydroxide in water was added and the temperature was slowly allowed to rise to $0^{\circ}C$. The solution stirred for 25 min and was washed down a florisil column with dichloromethane. The dichloromethane was removed on the rotary evaporator affording 60 mg of chlorobis(m-chlorobenzoato)bis(triphenylphosphine)iridium(III) (60%). This reaction was accompanied by the evolution of carbon dioxide which was identified by its mass spectrum and infrared spectrum.

Occasionally, a carbon monoxide-containing compound was obtained as a minor component from this reaction and the reaction of two equivalents of

m-chloroperoxybenzoic acid with Vaska's complex. This compound was identified as chlorobis(m-chlorobenzoato)carbonylbis(triphenylphosphine)iridium(III), and can be independently prepared from the reaction of m,m'-dichlorobenzoyl peroxide with Vaska's complex.

Other Reactions

Reaction of m,m'-Dichlorobenzoyl Peroxide with Vaska's Complex.

Vaska's complex (100 mg) was reacted with m,m'-dichlorobenzoyl peroxide (70 mg) in benzene under nitrogen overnight. A pale yellow solution was obtained. Ethanol was added and the volume was reduced until crystallization occurred. A white solid was obtained (90 mg, 62%).

Synthesis of Chloro(m-chlorobenzoato)hydridobis(triphenylphosphine)iridium(III)·H₂O. Trans-chloronitrogen bis(triphenylphosphine)iridium(I) (200 mg) was reacted with m-chlorobenzoic acid (100 mg) in carefully degassed benzene. After 2 h at room temperature, the solution changed from yellow to orange and hexane was added to precipitate the product. The powder was collected by filtration (50 mg, 21%).

Anal. calcd. for C₄₃H₃₅Cl₂O₂P₂Ir·H₂O: C, 55.72; H, 4.02. Found: C, 55.84; H, 3.88.

Reaction of Chloro(m-chlorobenzoato)hydridobis(triphenylphosphine)iridium(III) with m-Chloroperoxybenzoic Acid. Chloro(m-chlorobenzoato)hydridobis(triphenylphosphine)iridium(III) (20 mg) was reacted with m-chloroperoxybenzoic acid (1 equiv) in dichloromethane. The solution turned blue-green. Thin-layer chromatography (silica gel-dichloromethane) showed the absence of chloro bis(m-chlorobenzoato)bis(triphenylphosphine)iridium(III).

An infrared spectrum of the uncharacterizable product demonstrated the presence of triphenylphosphine oxide (1120 and 1160 cm^{-1}).

Reaction of Sodium Iodide and Chloro(p-methylbenzoato)carbonylbis-(triphenylphosphine)iridium(III)tetrafluoroborate. Chloro(p-methylbenzoato)-carbonylbis(triphenylphosphine)iridium(III)tetrafluoroborate (100 mg) in dichloromethane was added to an ethanolic sodium iodide solution. An orange precipitate formed as the dichloromethane was removed on the rotary evaporator. The solid was suction-filtered and washed with ethanol (90 mg, 87%). The infrared spectrum of this compound demonstrated loss of the carboxylato ligand, and resembled the infrared spectrum of chlorodiodo-carbonylbis(triphenylphosphine)iridium(III).

Reaction of Acetonitrile and Chloro(m-chlorobenzoato)carbonylbis-(triphenylphosphine)iridium(III)tetrafluoroborate. Chloro(m-chlorobenzoato)-carbonylbis(triphenylphosphine)iridium(III)tetrafluoroborate (100 mg) was dissolved in dichloromethane. Acetonitrile was added and the solution was heated until it turned colorless. Cyclohexane was added and white needles crystallized with evaporation of the dichloromethane. The solid was collected and washed with cyclohexane (70 mg, 67%). The infrared spectrum and ^1H NMR spectrum were consistent with chloro(m-chlorobenzoato)acetonitrilecarbonylbis(triphenylphosphine)iridium(III)tetrafluoroborate.

Reactions of Chloro(ethoxycarboxo)(p-methylbenzoato)bis(triphenylphosphine)iridium(III).

Reaction with Methyl Trifluoromethanesulfonate. Chloro(ethoxycarboxo)(p-methylbenzoato)bis(triphenylphosphine)iridium(III) (30 mg) was

dissolved with deuteriochloroform in an NMR tube. Slightly more than 1 equiv of methyl trifluoromethanesulfonate was added. The reaction was immediate and methyl ethyl ether was observed in the ^1H NMR spectrum. The volatiles were flash-distilled into another NMR tube. The infrared spectrum of the inorganic product was consistent with chloro(*p*-methylbenzoato)carbonylbis-(triphenylphosphine)iridium(III)trifluoromethanesulfonate or tetrafluoroborate.

Reaction with Trifluoromethane Sulfonic Acid. The previous procedure was repeated except trifluoromethane sulfonic acid was used instead of methyl trifluoromethanesulfonate. Ethanol was formed as the volatile component, and the inorganic product was chloro(*p*-methylbenzoato)-carbonylbis(triphenylphosphine)iridium(III)trifluoromethanesulfonate or tetrafluoroborate.

Reaction with Tert-butyl Isocyanide. Chloro(ethoxycarboxo)(*p*-methylbenzoato)bis(triphenylphosphine)iridium(III) (100 mg) was dissolved in dichloromethane and excess tert-butyl isocyanide was added. Ethanol was added after stirring 30 min, and the dichloromethane was removed on the rotary evaporator. A pale yellow solid was obtained (60 mg, 55%). The ^1H NMR and infrared spectra were consistent with chloro(ethoxycarboxo)*p*-methylbenzoato)(tert-butyl isocyanide)bis(triphenylphosphine)iridium(III).

Table 4

IR Data (cm ⁻¹)	Unidentate Carboxylato		Bidentate Carboxylato		Other	
	ν_a	ν_s	ν_a	ν_s		
IrCl(O ₂ CR) ₂ (PPh ₃) ₂	1649	1330	1494	1424		
IrCl(O ₂ CR) ₂ (CO)(PPh ₃) ₂	1658	1330	--	--	$\nu(\text{C}\equiv\text{O})$	2070
[IrCl(O ₂ CR')(CO)(PPh ₃) ₂] BF ₄	--	--	1480	1435	$\nu(\text{BF}_4)$ $\nu(\text{C}\equiv\text{O})$	1055 2070 (soln), 2080, 2070 (nujol)
[IrCl(O ₂ CR)(CO)(PPh ₃) ₂] BF ₄	--	--	1485	1435	$\nu(\text{BF}_4)$ $\nu(\text{C}\equiv\text{O})$	1055 2080
IrCl(CR''O)(O ₂ CR')(PPh ₃)			1485	1425	$\nu(\text{C}=\text{O})$ $\nu(\text{C}-\text{O})$	1653 1040
IrCl(¹³ CR''O)(O ₂ CR')(PPh ₃) ₂	--	--	1485	1425	$\nu(\text{C}=\text{O})$ $\nu(\text{C}-\text{O})$	1615 1030
IrCl(CNH ₂ O)(O ₂ CR)(PPh ₃) ₂	--	--	1485	1420	$\nu(\text{C}=\text{O})$ $\nu(\text{amide})$ $\nu(\text{NH}_2)$	1611 1580 3500, 3370

Table 4. Continued

IR Data (cm ⁻¹)	Unidentate Carboxylato		Bidentate Carboxylato		Other	
	ν_a	ν_s	ν_a	ν_s		
IrCl(¹³ CNH ₂ O)(O ₂ CR)(PPh ₃) ₂	--	--	1485	1420	ν (C=O) ν (amide) ν (NH ₂)	1558 1546 3500, 3370
IrCl(O ₂ CR)H(PPh ₃) ₂	--	--	1480	1435	ν (Ir-H)	2270
IrClI ₂ (CO)(PPh ₃) ₂	--	--	--	--	ν (C≡O)	2070
IrCl(O ₂ CR')(CR''O)(CNR''')(PPh ₃) ₂	1635	1330	--	--	ν (C=O) ν (C-O) ν (NC)	1650 1045 2190
[IrCl(O ₂ CR')(CH ₃ CN)(CO)(PPh ₃) ₂]BF ₄	1610	1330	--	--	ν (CN) ν (C≡O) ν (BF ₄)	2320 2100 1050

R = m-chlorobenzoato
R' = p-methylbenzoato
R'' = ethoxy
R''' = tert-butyl

Table 5. ^1H NMR Data (CDCl_3).

	Chemical Shift (δ) and Coupling Constants			
$[\text{IrCl}(\text{O}_2\text{CR}')(\text{CO})(\text{PPh}_3)_2]\text{BF}_4$	2.25	s	3H	Me
	6.9-8.0	m	34H	Ph
$[\text{IrCl}(\text{O}_2\text{CR}')(\text{CH}_3\text{CN})(\text{CO})(\text{PPh}_3)_2]\text{BF}_4$	2.1	s	3H	Me
	2.3	s	3H	Me
$\text{IrCl}(\text{O}_2\text{CR}')(\text{CR}''\text{O})(\text{CNR}''')(\text{PPh}_3)_2$	0.8	t	3H	$^3J_{\text{H-H}}$ 7 Hz
	1.1	s	9H	
	2.25	s	3H	
	3.25	q	2H	$^3J_{\text{H-H}}$ 7 Hz
	7.0	m	30H	
$\text{CH}_3\text{OCH}_2\text{CH}_3$	1.2	t	3H	$^3J_{\text{H-H}}$ 7 Hz
	3.3	s	3H	
	3.4	q	2H	$^3J_{\text{H-H}}$ 7 Hz

R' = p-methylbenzoato

R'' = ethoxy

R''' = tert-butyl

References and Notes

- (1) (a) Kwart, H.; Hoffman, D. M. J. Org. Chem. **1966**, 31, 419. (b) Mimoun, H. Angew. Chem. Int. Ed. **1982**, 21, 734.
- (2) (a) Bartlett, P. D. Rec. Chem. Prog. **1957**, 18, 111. (b) Taseuki, M.; Azman, A. J. Am. Chem. Soc. **1978**, 100, 743.
- (3) Collman, J. P.; Kubota, M.; Vastine, F. D.; Sun, J. Y.; Kung, J. W. J. Am. Chem. Soc. **1968**, 90, 5430.
- (4) Schlodder, R.; Ibers, J. A.; Lenarda, M.; Graziani, M. J. Am. Chem. Soc. **1974**, 96, 6893.
- (5) (a) Ugo, R.; Conti, F.; Cenini, S.; Mason, R.; Robertson, G. B. J. Chem. Soc., Chem. Commun. **1968**, 1498. (b) Ugo, R.; Zanderighi, G. M.; Fusi, A.; Carreri, D. J. Am. Chem. Soc. **1980**, 102, 3745. (c) Sheldon, R. A.; van Doorn, J. A. J. Organomet. Chem. **1975**, 94, 115.
- (6) Walker, J. A.; Knobler, C. B.; Hawthorne, M. F. J. Am. Chem. Soc. **1983**, 105, 3370.
- (7) Bird, C.; Booth, B. L.; Haszeldine, R. N.; Neuss, G. R. H.; Smith, M. A. J. Chem. Soc., Dalton Trans. **1982**, 1109.
- (8) Atlay, M. T.; Preece, M.; Strukul, G.; James, B. R. J. Chem. Soc., Dalton Trans. **1982**, 406.
- (9) Booth, B. L.; Haszeldine, R. N.; Neuss, G. R. H. J. Chem. Soc., Dalton Trans. **1972**, 1074.
- (10) Bird, C.; Booth, B. L.; Haszeldine, R. N. J. Chem. Soc., Dalton Trans. **1982**, 517.
- (11) Harvie, I. J.; McQuillin, F. J. J. Chem. Soc., Dalton Trans. **1976**, 369.
- (12) Booth, B. L.; Haszeldine, R. N.; Neuss, G. R. H. J. Chem. Soc.,

- Perkin Trans. **1975**, 209.
- (13) Booth, B. L.; Haszeldine, R. N.; Neuss, G. R. H. J. Chem. Soc., Dalton Trans. **1982**, 511.
- (14) Booth, B. L.; Haszeldine, R. N.; Neuss, G. R. H. J. Chem. Soc., Dalton Trans. **1982**, 37.
- (15) Fusi, A.; Ugo, R.; Fox, F.; Pasini, A.; Cenini, S. J. Organomet. Chem. **1971**, 26, 417.
- (16) Fusi, A.; Ugo, R.; Zanderrighi, G. M. J. Catal. **1974**, 34, 175.
- (17) Fusi, A.; Capperalla, G. Inorg. Nucl. Chem. Lett. **1972**, 8, 127.
- (18) Kurkov, V. P.; Pusky, J. Z.; Lavighe, J. B. J. Am. Chem. Soc. **1968**, 90, 4743.
- (19) Fine, L. W.; Grayson, M.; Suggs, V. H. J. Organomet. Chem. **1970**, 22, 219.
- (20) Lyons, J. A.; Turner, J. O. J. Org. Chem. **1972**, 37, 2881.
- (21) Lyons, J. A.; Turner, J. O. Tetrahedron Lett. **1972**, 29, 2903.
- (22) Sheldon, R. A. Chem. Commun. **1971**, 788.
- (23) Nakamoto, K. "Infrared and Raman Spectra of Inorganic and Coordination Compounds"; John Wiley and Sons: New York, 1978; p. 232.
- (24) (a) Angelici, R. J. Accts. Chem. Res. **1972**, 5, 335. (b) Kang, H. C.; Mauldin, C. H.; Cole, T.; Slegeir, W.; Pettit, R. J. Am. Chem. Soc. **1977**, 99, 8323. (c) Laine, R. M.; Rinker, R. G.; Ford, P. C. Ibid. **1977**, 99, 252. (d) Ungermann, C.; Landis, U.; Moya, S. A.; Cohen, H.; Walker, H.; Pearson, R. G.; Rinker, R. G.; Ford, P. C. Ibid. **1979**, 101, 5922. (e) Cheng, C. H.; Hendrickson, D. E.; Eisenberg, R.

- Ibid. 1977, 99, 2791. (f) King, R. B.; Frazier, C. C.; Hanes, R. M.; King, A. D. Ibid. 1978, 100, 2925. (g) Angelici, R. J.; Busetto, L. Ibid. 1969, 91, 3197. (h) Werner, H.; Beck, W.; Engelmann, H. Inorg. Chim. Acta 1969, 3, 331.
- (25) Stewart, R. F.; Davidson, E. R.; Simpson, W. T. J. Chem. Phys. 1965, 42, 3157.
- (26) "International Tables for X-ray Crystallography, Vol. IV"; Kynoch Press: Birmingham, England, 1974; p. 155.
- (27) $R = \{ \sum |kF_o| - |F_c| / \sum |kF_o| \}$ and G.O.F. = $\{ w(F_o^2 - F_c^2)^2 / (n_o - n_p) \}^{1/2}$ where n_o is the number of reflections and n_p is the number of parameters. All atomic coordinates were in one block, and the scale factor, k , and the Gaussian ellipsoids (isotropic for all atoms except iridium, chlorine, P₁, P₂, O₁, O₂, CT₁, O, B, F₁, F₂, F₃, and F₄) in the other. Hydrogen atoms were placed a distance of 0.98 Å from their respective carbon atom by assuming ideal geometry, and were not refined.
- (28) Swain, G. G.; Stockmayer, W. H.; Clarke, J. T. J. Am. Chem. Soc. 1950, 72, 5426.
- (29) Carothers, W. H. "Organic Syntheses, Vol. 13"; John Wiley and Sons, Inc.: New York, 1933; p. 86.